IOSUD – UNIVERSITY „DUNĂREA DE JOS" OF GALAȚI

The School of Doctoral Studies in Mechanical and Industrial Engineering

SUMMARY

PHD THESIS

STUDIES CONCERNING THE STRUCTURAL RISK ANALYSIS FOR ACCIDENTAL LOADS OF SHIPS

PhD Student,
Eng. Dumitru-Silviu PERIJOC

Scientific supervisor,
Prof.univ.dr.eng. Leonard DOMNIȘORU

Series I 6: Mechanical Engineering No. 81
GALAȚI
2024

IOSUD – UNIVERSITY „DUNĂREA DE JOS" OF GALAȚI

The School of Doctoral Studies in Mechanical and Industrial Engineering

SUMMARY

PHD THESIS

STUDIES CONCERNING THE STRUCTURAL RISK ANALYSIS FOR ACCIDENTAL LOADS OF SHIPS

PhD Student,
Eng. Dumitru-Silviu PERIJOC

President	Prof.univ.dr.eng. Elena MEREUȚĂ
Scientific supervisor,	Prof.univ.dr.eng. Leonard DOMNIȘORU
Scientific reviewers,	Prof.univ.dr.eng. H.C. Anton HADĂR Prof.univ.dr.eng. Ioan Călin ROȘCA Prof.univ.dr.eng. Costel Iulian MOCANU

Series I 6: Mechanical Engineering No. 81
GALAȚI
2024

TABLE OF CONTENTS

Introduction

Context and Motivation

In the naval industry, the safety and durability of ship structures are essential priorities, especially for inland navigation vessels such as barges. Inland navigation conditions include variable depths, strong currents, and the presence of underwater obstacles, factors that can lead to grounding incidents. Although initially minor, these incidents can escalate into severe structural damages, with significant economic and ecological consequences. In this context, assessing the impact of ship groundings has become a crucial component of structural safety analysis.

The increasing frequency of groundings in recent decades underscores the need for detailed studies that address both the structural integrity in an intact state and the behavior under accidental loads. Statistical data provided by authorities such as the European Maritime Safety Agency (EMSA) and the Romanian Naval Authority (ANR) indicate that groundings represent a significant percentage of total maritime accidents, with barges often being involved, having the highest causality.

Studies on the structural impact of groundings are gaining increased importance to understand how ship movements influence structural behavior and the risk of damage. These studies contribute to the development of design strategies aimed at enhancing structural resilience and reducing the risk of collapse in the event of an impact.

Grounding can introduce extreme stresses into the ship's hull, and the nature and severity of these stresses depend on several factors, including the ship's geometry and the characteristics of the seabed on which it grounds. Traditional approaches, based on simplified models, are not always sufficient to capture all relevant aspects of structural behavior. Therefore, integrating advanced numerical simulation techniques, such as the Finite Element Method (FEM), becomes essential for accurate and comprehensive assessment.

Recent advances in numerical simulation and increased computational capacity allow for much more detailed and precise analyses, including the simulation of complex grounding scenarios. Numerical simulations are essential for optimizing ship structures to make them more resistant to groundings.

Beyond technical aspects, there are also strong economic and ecological motivations for improving structural risk assessment methods. Severe grounding incidents can generate significant material losses as well as major ecological damage. Developing advanced structural analysis methods can significantly reduce the risk of such incidents, contributing to the increased safety and durability of naval structures.

Objectives of the thesis

The thesis aims to address the critical issues related to the assessment of the structural strength and dynamic behavior of inland waterway vessels, with a focus on the impact at grounding. The objectives are formulated to provide an in-depth understanding of these issues using advanced numerical simulation and experimental validation methods.

1. Assessment of overall intact strength

The first major objective is to assess the global intact strength of inland navigation vessels. This involves the use of three-dimensional models (3D-FEM) to represent the geometry and mass distribution of the vessel to identify critical stress points and to assess the structural ability to withstand various loading conditions.

2. Assessment of ship dynamics

The second objective is the assessment of ship dynamics, which is essential to understand the ship's behavior under various sailing conditions. This study involves the analysis of heave, pitch and roll motions influenced by hull shape and operating conditions. Advanced numerical simulation methods will be used to model this dynamic behavior.

3. Impact assessment from grounding in calm water

Another major objective is the analysis of the structural behavior of the ship under grounding conditions, such as collisions with underwater obstacles or impact with the bottom of the waterway. Advanced numerical simulations will allow the identification of damage modes and the assessment of their impact on structural integrity.

4. Impact assessment from grounding considering ship dynamics in waves

The last objective is to integrate the ship dynamics into the grounding impact analysis, considering the influence of the ship motions on the structural behavior during impact. Advanced numerical models will simulate the interaction between ship dynamics and structural impact in grounding scenarios.

Structure of the thesis

Chapter 1 presents the current state of the research and the background necessary to understand the importance of the assessment of the impact of grounding. It discusses the motivation for the study and the objectives of the thesis, emphasizing the relevance of the research to inland navigation and ship structural safety.

Chapter 2 presents the theoretical and numerical underpinnings used in the assessment of the structural strength of ships, with a focus on global and local analysis of structures using 3D-FEM models, as well as structural impact analysis. It also discusses the fundamentals for analyzing ship dynamics in regular and random wave oscillations using various hydrodynamic models.

Chapter 3 explores the validation of theoretical models by physical experiments. The results of numerical simulations are compared with experimental data to ensure the accuracy and reliability of the models used in structural impact assessment and ship oscillation dynamics.

Chapter 4 presents the overall strength analysis of a 3000 TDW river barge using 1D and 3D-FEM models. Structural stresses and deformations under various loading scenarios are evaluated, providing a detailed insight into the global and local structural behavior in equivalent design oblique waves.

Chapter 5 presents the analysis of the overall strength of a 24 m long GRE composite river-coastal craft on 3D-FEM models in equivalent design oblique design waves. The chapter also includes experimental determination of two types of GRE composite materials and selection of the most suitable structural variant.

Chapter 6 presents the oscillation dynamics analysis of a 3000 TDW river barge using two hydrodynamic models in regular waves. Short-term statistical analysis of the dynamic response in random oblique waves is also carried out, highlighting the safety limits in navigation.

Chapter 7 analyzes the oscillation dynamics for a GRE composite river-coastal craft in regular waves. The analysis includes a navigational safety assessment and provides kinematic parameters for the grounding impact study.

Chapter 8 deals with stranding impact assessment in both calm water and wave conditions. Critical points of failure and damage modes are analyzed, using advanced numerical simulations to determine the structural response of the ship in the event of a grounding impact. Comparative analyses are performed for several navigation scenarios, for a 3000 TDW barge and a composite craft.

Chapter 9 summarizes the conclusions of the thesis, highlighting the importance of integrating advanced modeling methods in the assessment of structural risk in ship grounding and proposes future research directions.

Current state of research

1.1. Accidental loads and damage in ship operations

Marine casualties, such as collisions and groundings, remain a major cause of structural losses and environmental disasters. Statistical studies show that groundings have contributed significantly to marine casualties, causing structural damage and material losses [1], [2]. Recent examples include the grounding of the bulk carrier MV Wakashio [3] on the coral reef of Mauritius and the collision of the oil tanker SANCHI [4], which resulted in fuel spills and loss of life. Another notable incident is that of the Exxon Valdez oil tanker [5], which caused a massive oil spill in Alaska, affecting thousands of kilometers of coastline. Such accidents underline the need for preventive measures and in-depth research into structural damage and its impact on the environment.

Tabel 1.1. Main causes of maritime accidents – 2019.[1]

Accident cause	%
Loss of control	30
Collision	16
Contact	16
Equipment failure	14
Grounding	13
Fire/Explosion	6
Flooding	3
Heel	1
Structural collapse	1

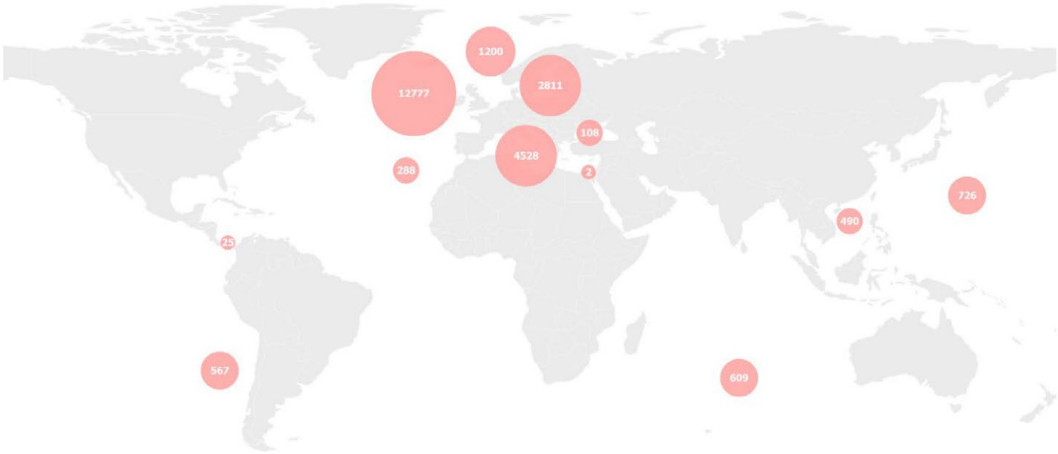

Figure 1.1. The global situation of maritime accidents.[2]

1.2 Current state of research on ship grounding mechanics

Recent research has made significant advancements in the mechanics of ship grounding. Pedersen (1994)[6] and Simonsen (1997)[7] developed mathematical models that assess the impact of grounding on ship structures. These models identify the shear forces and bending moments that may occur during grounding and how they exceed the allowable structural limits. Moreover, advanced numerical methods, such as FEM (Finite Element Method), provide the ability to simulate groundings for large ships and have become an essential tool in assessing structural capacity. Kitamura (2002) [8] demonstrated the effective use of nonlinear numerical simulations in impact and grounding studies.

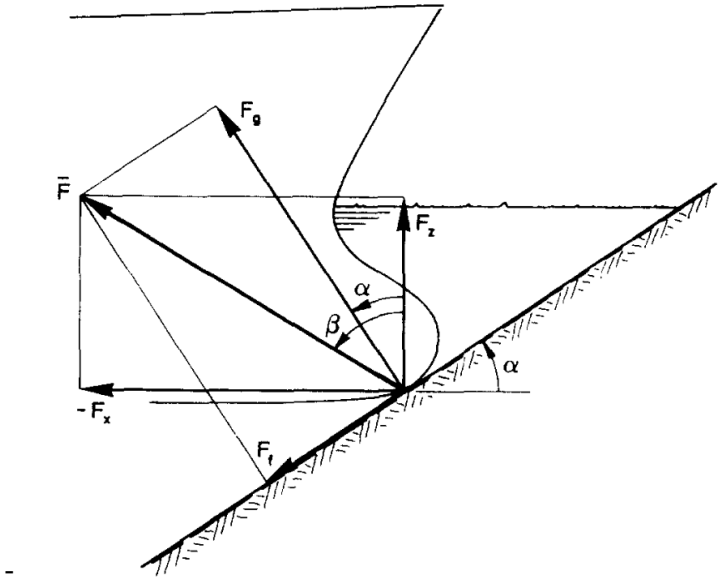

Figure 1.2 Resultant forces due to the initial impact.[6]

Additionally, the research by Alsos and Amdahl (2007) [9] demonstrated the critical impact that groundings on large contact surfaces, such as sandbanks, can have on ships, damaging structural elements and reducing overall load-carrying capacity. More recently, Nguyen et al. (2011) [10] developed a general model for evaluating ship groundings, integrating the longitudinal and vertical movements of the ship into their analyses.

1.3 Maritime classification societies' rules for assessing structural capability under accidental loads

Classification societies, such as DNV [11] and Bureau Veritas [12], have developed strict regulations regarding the assessment of structural strength in the event of accidental loads, including groundings and collisions. Their regulations establish requirements for the minimum thickness of plates and structural members, as well as for periodic inspections to ensure compliance with established standards. For example, DNV rules specify that ships must be capable of withstanding the bending moments and shear forces generated during a grounding. Similarly, other societies, such as Bureau Veritas, impose rules for designing structures to resist accidental loads. These regulations are essential for preventing structural collapse [1], [2] and ensuring the safety of ships in operation.

1.4 National context regarding recorded maritime accidents in Romania

In Romania, maritime accidents are monitored by the Romanian Naval Authority (ANR) [13], which annually reports incidents within territorial waters. Groundings are the most frequent type of maritime accident, with over 60 reported cases, highlighting the vulnerability of vessels, particularly barges, to such incidents. Other frequently reported accidents include collisions between ships and port infrastructures. Romanian ports, such as Constanța and Galați, register the highest number of groundings, especially in areas with heavy maritime traffic. This high frequency of accidents underscores the need for additional preventive measures and research into the effects of groundings on the structural integrity of ships.

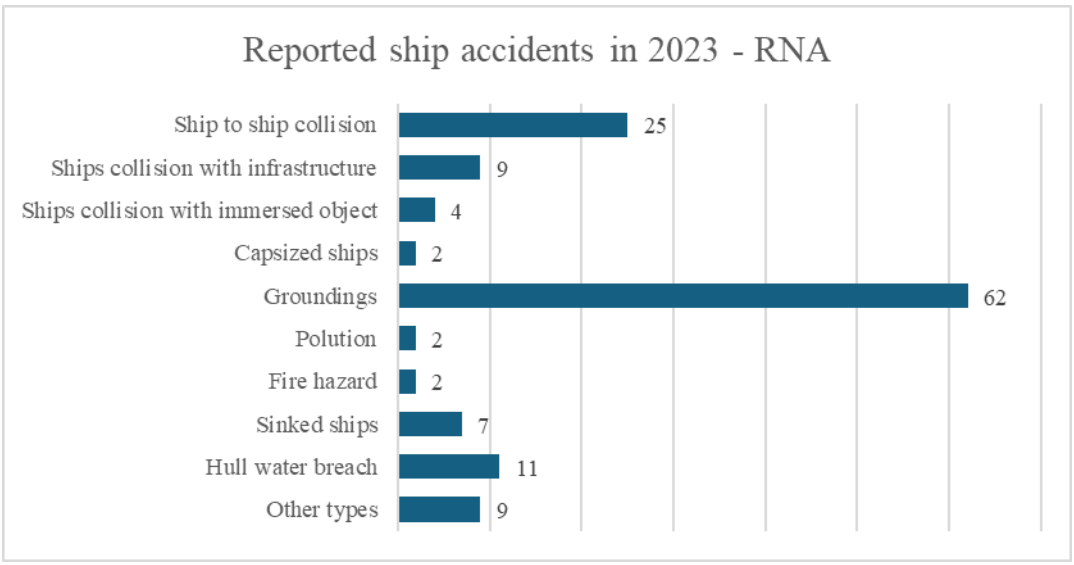

Figure 1.3 The situation of maritime accidents in Romania's territorial waters - 2023. ANR Report.[13]

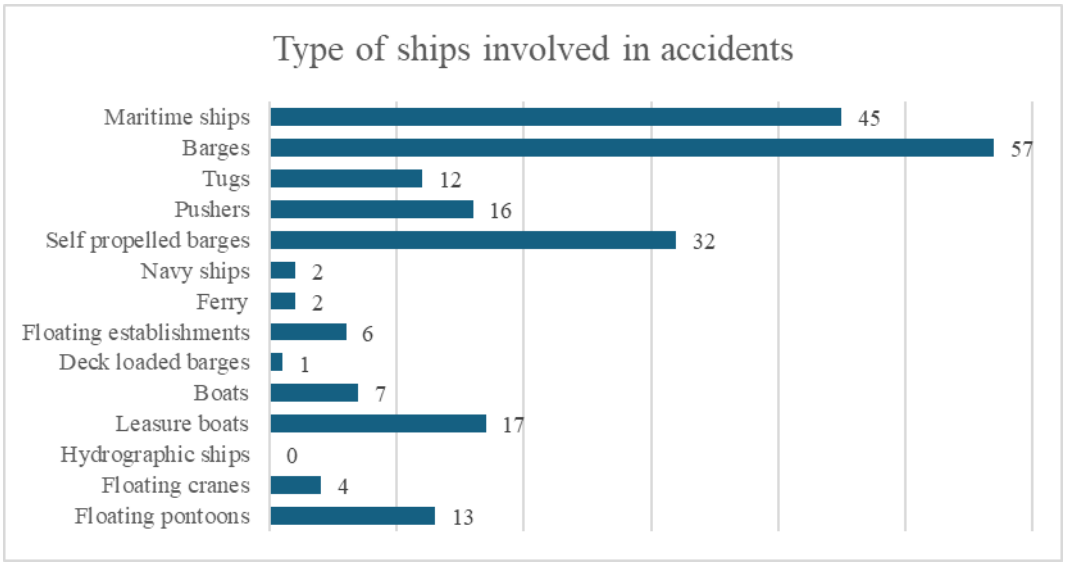

Figure 1.4 Types of ships involved in accidents - 2023. ANR Report.[13]

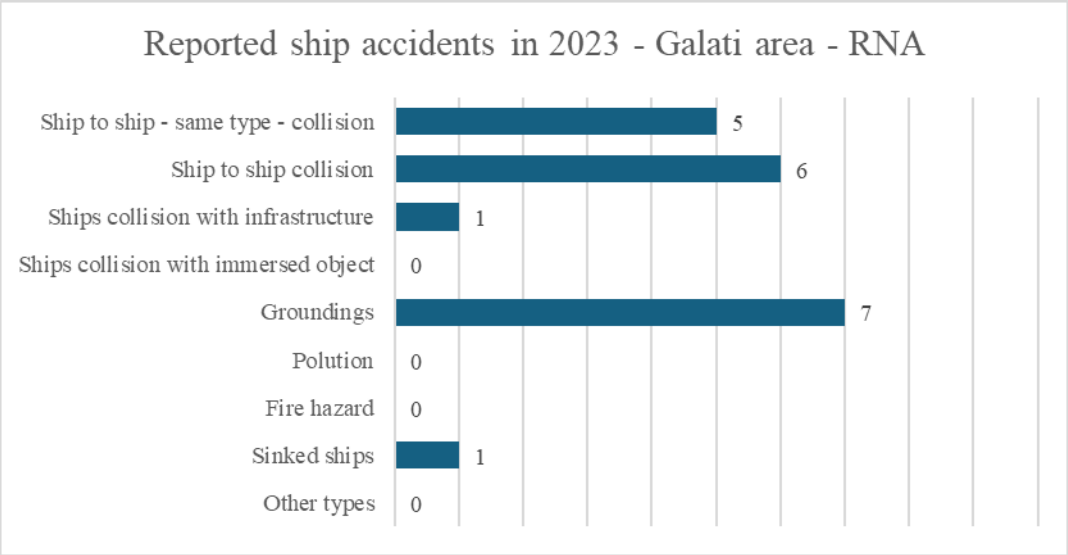

Figure 1.5 The situation of maritime accidents in the Galați port area - 2023. ANR Report [13]

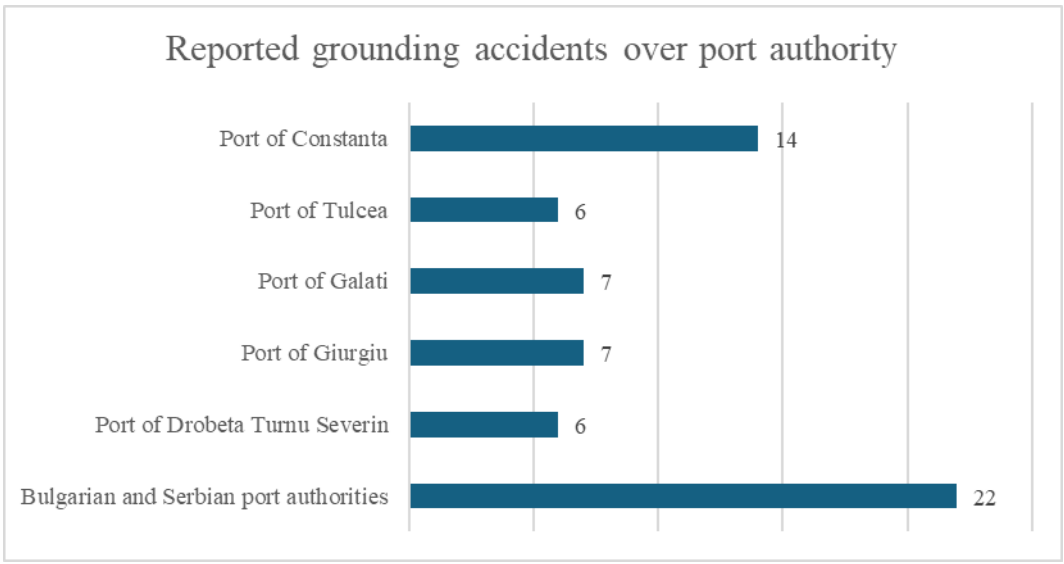

Figure 1.6 The situation of groundings recorded by port authorities - 2023. ANR Report.[13]

Chapter 2

THEORETICAL FOUNDATIONS. GLOBAL AND LOCAL RESISTANCE, OSCILLATIONS, SHIP IMPACT

2.1 Stages of 3D-CAD/FEM modeling of a ship structure

This section describes the essential steps for creating a detailed structural model of a ship using CAD software and the finite element method (FEM). 3D-CAD/FEM modeling is crucial for accurately assessing the structural behavior of ships and finding a balance between the level of detail and the available computational power. Different sections of the ship are developed separately, and the structure is then combined into a global model.

2.1.1 Generating the Ship Hull Surfaces

The modeling process begins with generating the external surfaces of the ship’s hull. These are created based on the lines plan and the preliminary structural arrangement, using advanced CAD software such as Ansys SpaceClaim. This stage enables the creation of an accurate geometry, which can later be used for finite element discretization.

2.1.2 Generating Structural Element Surfaces

Next, the internal structural surfaces, such as bulkheads, the framing, and the ship’s stiffeners, are generated based on the construction drawings. HP-type profiles are equivalently modeled as L-type profiles, as used in the design, in accordance with classification society requirements. This step ensures that the modeled structure complies with the imposed strength requirements.

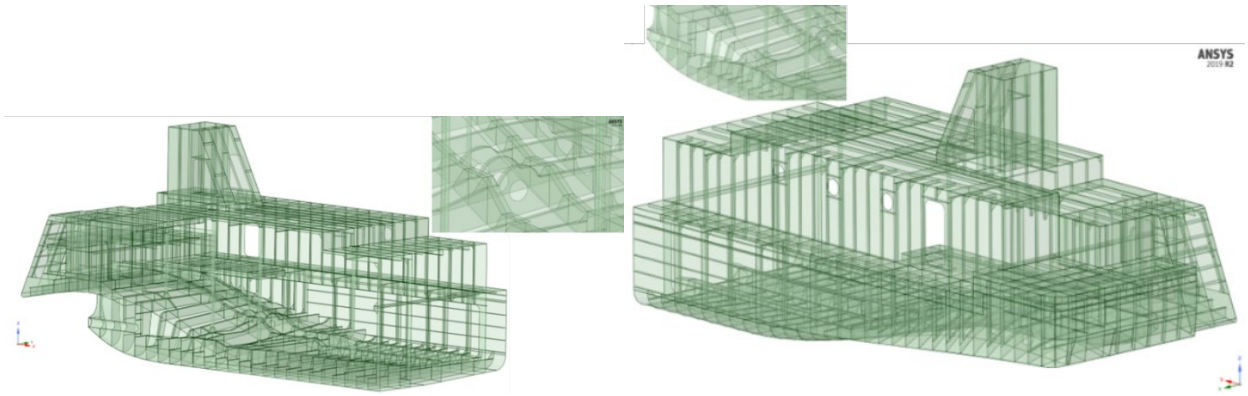

Figure 2.1. Typical CAD model. Stern area, river pusher.[14]

Tabel 2.1. Equivalence of HP profiles to L-angle profiles.[14]

HP Profile *Type*	Equivalent L-profile *H x W x t [mm]*
HP 80x6	80 x 20 x 6
HP 80x7	80 x 20 x 7
HP 100x7	100 x 25 x 7
HP 120x7	120 x 30 x 7

2.1.3 Developing the 3D-CAD Model in Block Sections

The ship's CAD model is developed in separate sections for the stern, midship, and bow areas to simplify the management of details. This modular process allows for a detailed and manageable analysis of each section before the final assembly of the entire model.

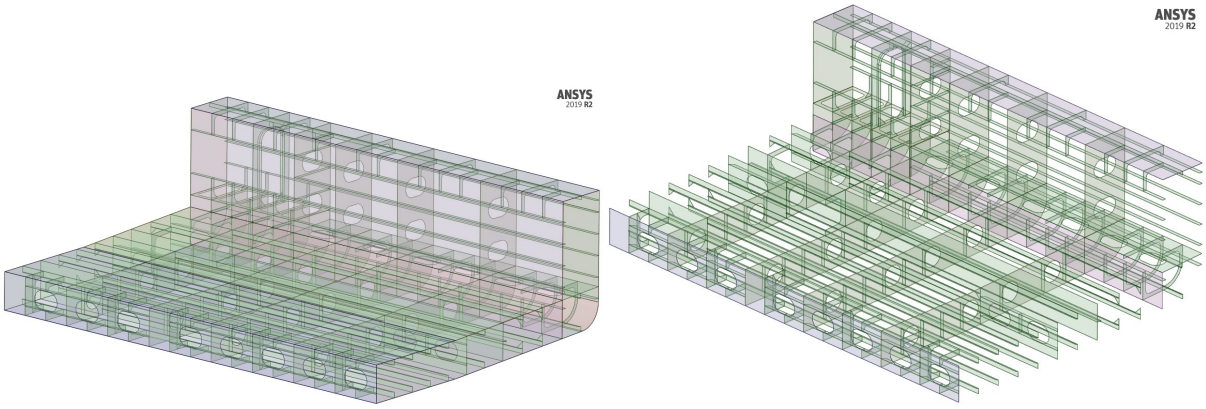

Figure 2.2 Typical CAD model. Midship area, river pusher.[14]

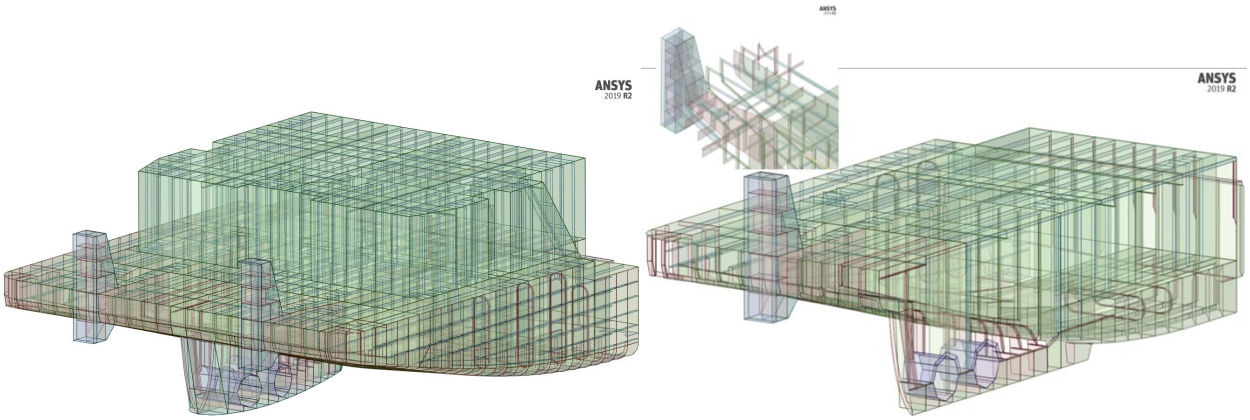

Figure 2.3 Typical CAD model. Bow area, river pusher.[14]

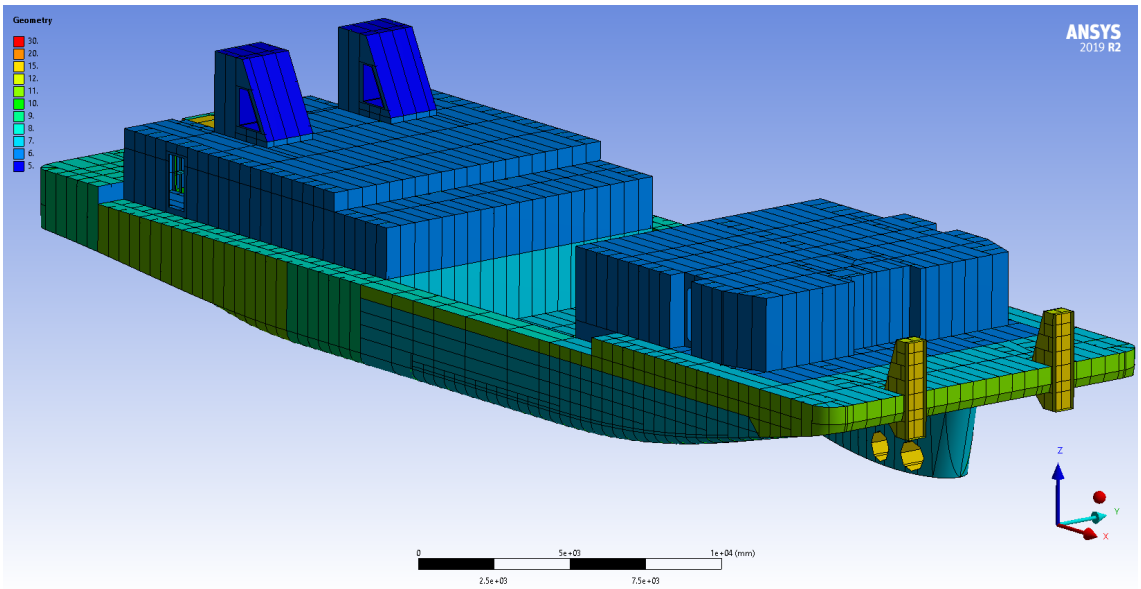

Figure 2.4 Assembled 3D-CAD model, river pusher, color plot - thicknesses. [14]

2.1.4 Developing the 3D-FEM Model for the Ship Hull

Once the CAD model is completed, it is discretized using finite elements, which are essential for performing structural analyses. This step allows for a detailed analysis of the ship's structural behavior under various loading conditions, including groundings and impacts. The size of the finite element discretization is selected according to the requirements of classification societies and industry best practices to ensure the accuracy of the analysis.

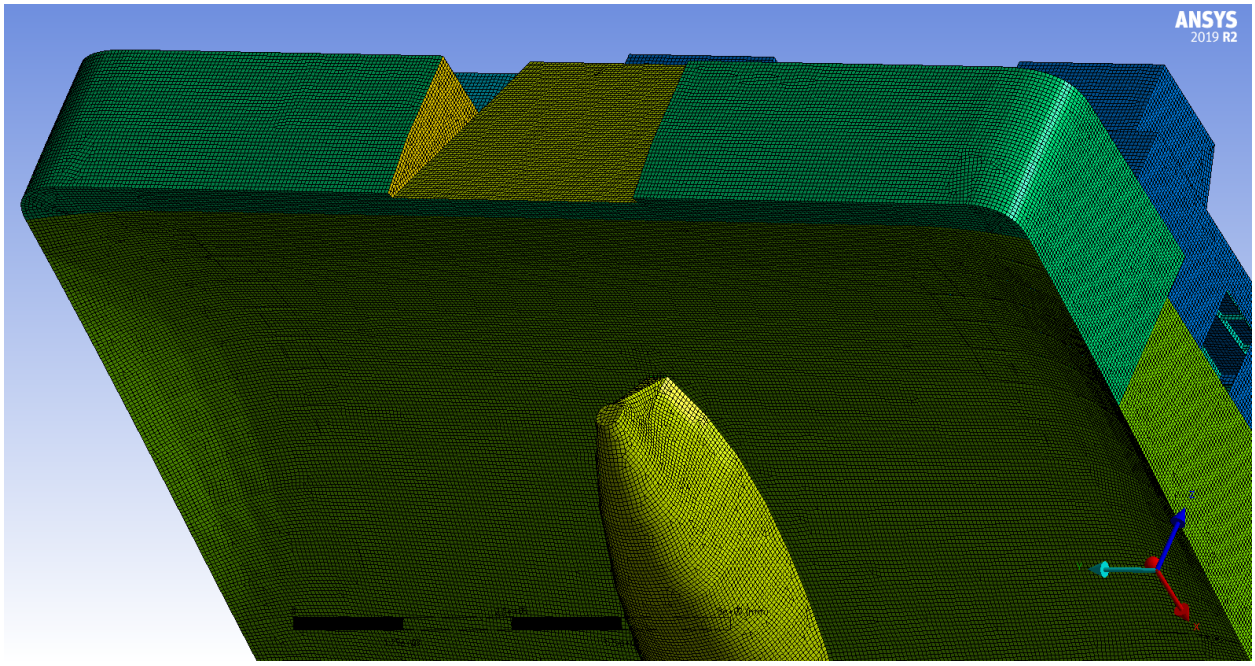

Figure 2.5 3D-FEM model, stern, river pusher. [14]

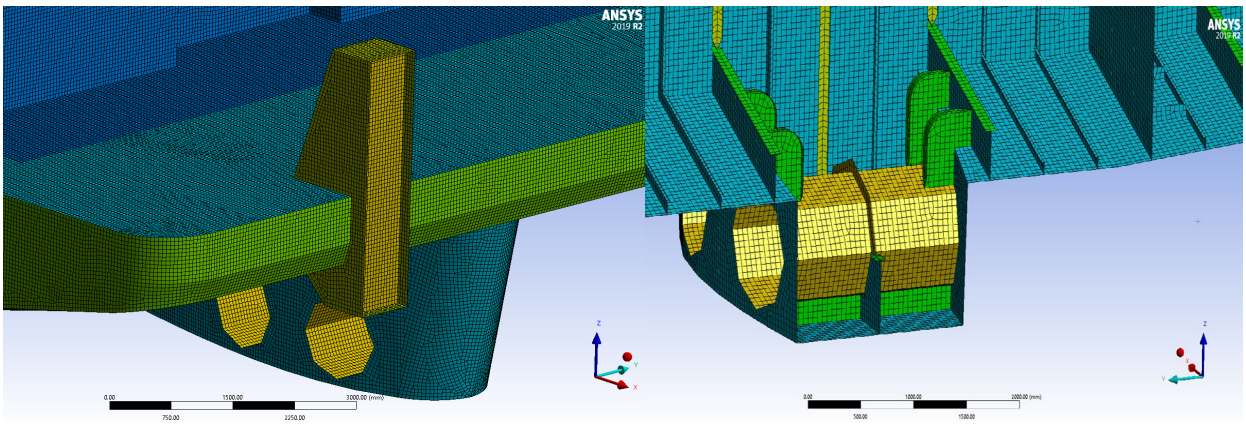

Figure 2.6 3D-FEM model, bow, river pusher. [14]

2.2 Methods of analyzing the global and local resistance of ships

This section describes the methods used to analyze the global and local strength of ship structures. A combined approach of 1D and 3D methods is presented, allowing for the evaluation of the ship's structural behavior under various operating conditions. FEM models are used to simulate the loads and forces acting on the ship during normal operation and in extreme conditions, such as large waves or impacts. The 3D FEM models are combined with hydrostatic and hydrodynamic evaluations to determine critical points of stress and deformation.

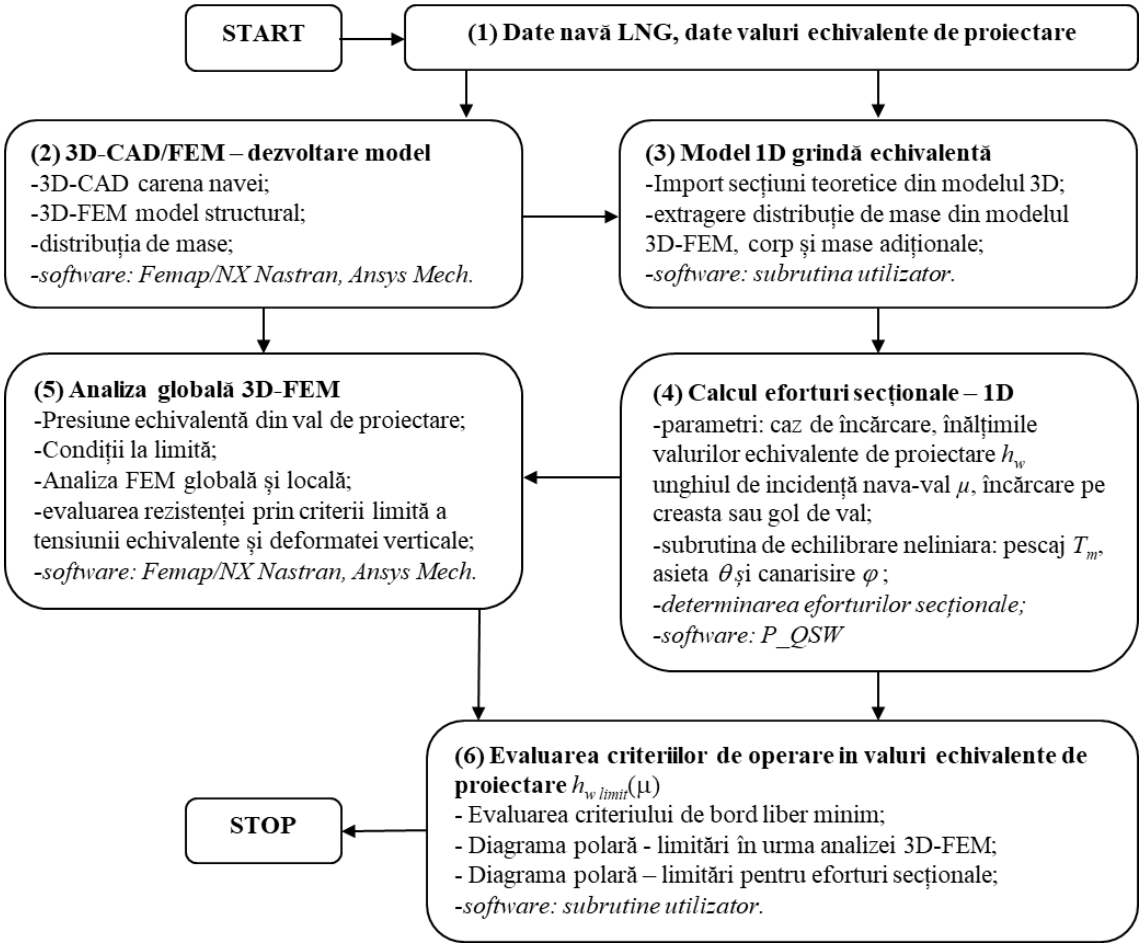

Figure 2.7 Algorithm for global and local 1D-3D/FEM analysis of a ship's hull structure. [15], [16]

2.3 Methods for evaluating ship motions (oscillations) – regular and random waves

The ship's movements in waves are analyzed using numerical methods that assess the hydrodynamic performance of the vessel. This section describes two methods used to evaluate oscillations: the strip method and the boundary element method. Both methods are employed to analyze the ship’s oscillations in regular and random waves, providing essential information about the ship's stability and behavior under various operating conditions.

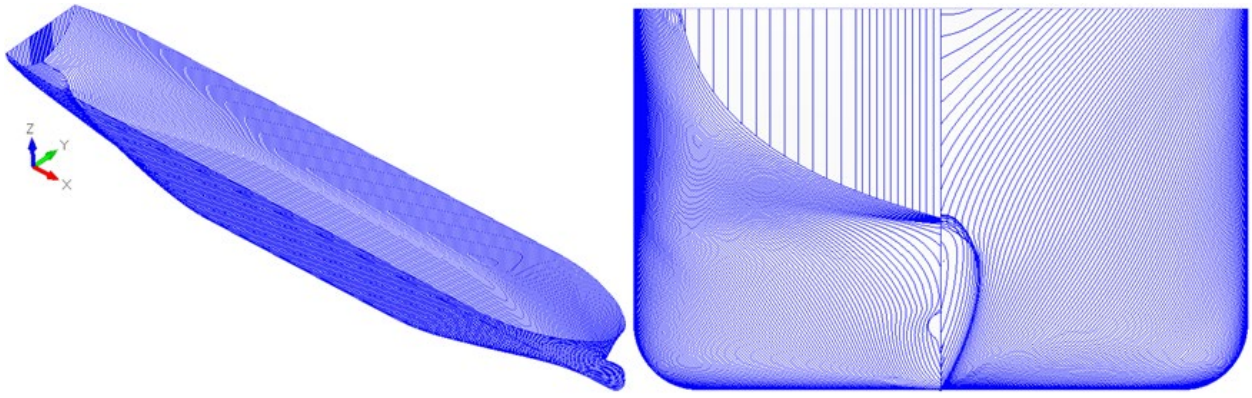

Figure 2.8 3D-CAD model. Hull lines plan. LNG tanker.[16]

2.3.1 Ship motion analysis using the transverse section method

The strip method is used to evaluate the primary motions of the ship, such as vertical translation, roll, and pitch. It allows for the calculation of the response amplitude operators (RAO) in regular waves and the assessment of the ship’s motions under varying wave intensities. This method is frequently used for monohull ships and provides a balance between the accuracy of results and computational requirements.

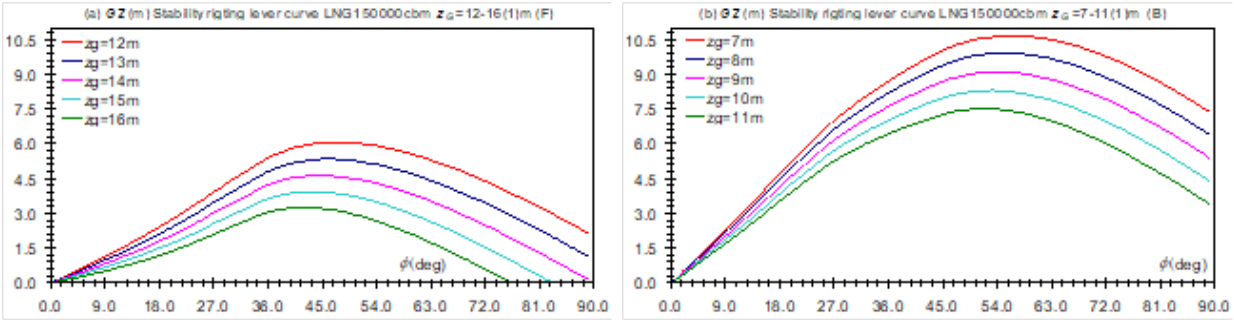

Figure 2.9 Transverse stability diagrams. LNG tanker. [15], [17]

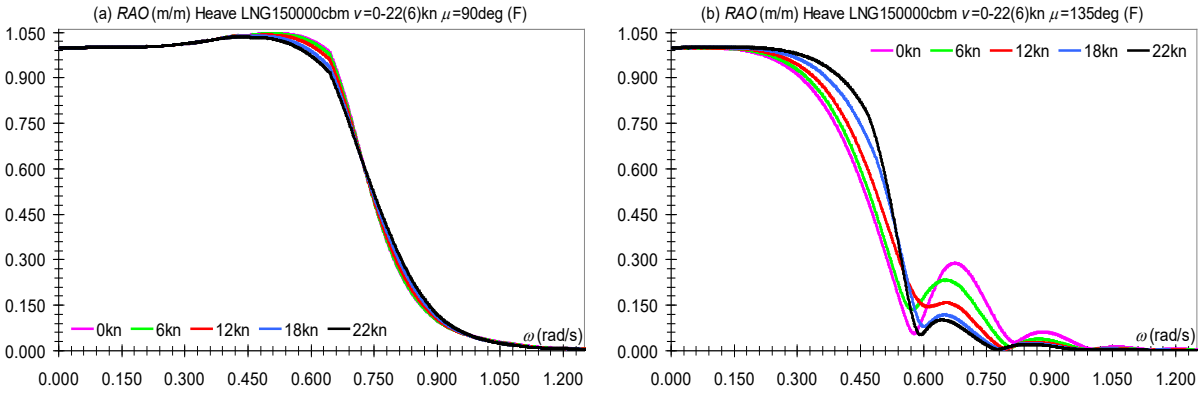

Figure 2.10 Response amplitude operators for oscillations. Vertical motion. LNG tanker, full load case. [15], [17]

2.3.2 Ship motion analysis using the boundary element method – Ansys Aqwa

The boundary element method is used to assess the effects of hydrodynamic loads on the ship, utilizing Ansys Aqwa software. This method allows for the evaluation of the ship’s movements under the influence of waves, currents, and wind, providing a detailed assessment of the ship’s structural behavior in varying environmental conditions. Both regular and irregular waves are used in this analysis, modeled with the help of ITTC spectra.

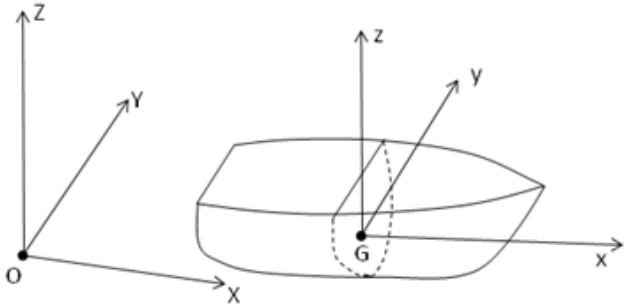

Figure 2.11 Definition of the coordinate system. [18]

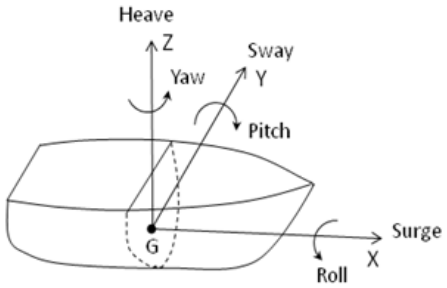

Figure 2.12 Definition of ship motions relative to the coordinate system. [18]

2.4 Preliminary methods for calculating impact stresses on structures

This section presents the preliminary methods used to evaluate the structural stresses generated by impacts. Numerical simulations are conducted using the Femap NX/Nastran code and the Advanced Nonlinear Explicit solver to assess the behavior of steel plates, with and without stiffeners, following impact with rigid or deformable objects. Evaluations include analyses for various impact speeds, and the results are presented in the form of graphs illustrating total contact forces, von Mises stress distributions, and structural deformations. These analyses are essential for determining critical points of structural failure and for developing optimal design solutions that ensure the integrity of the ship under impact conditions.

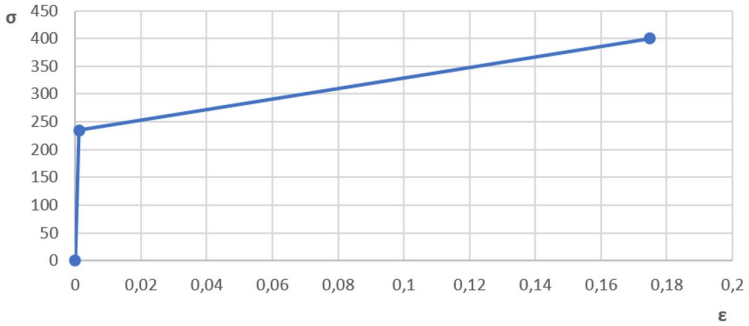

Figure 2.13 Stress-strain relationship. [19]

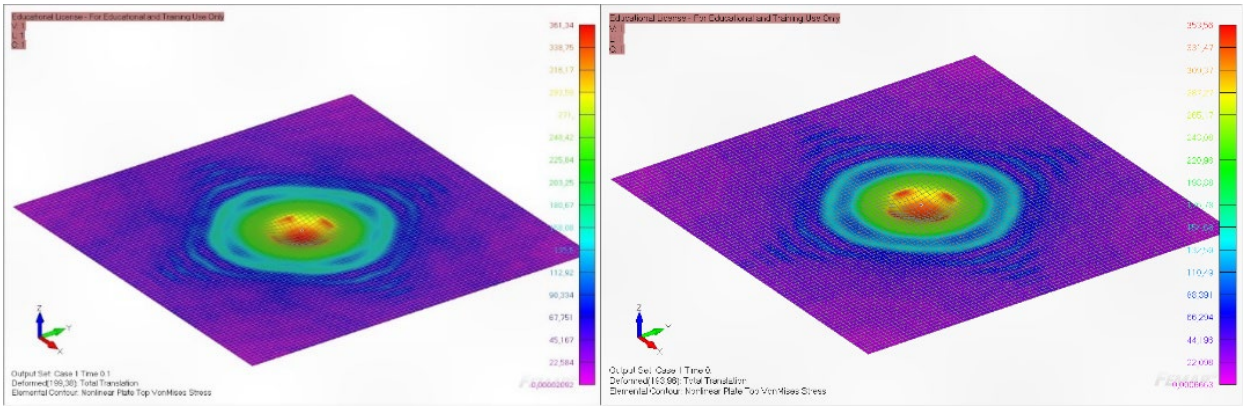

Figure 2.14 Case 2 (left). Case 5 (right). Simple plate. Von Mises stresses upon impact.

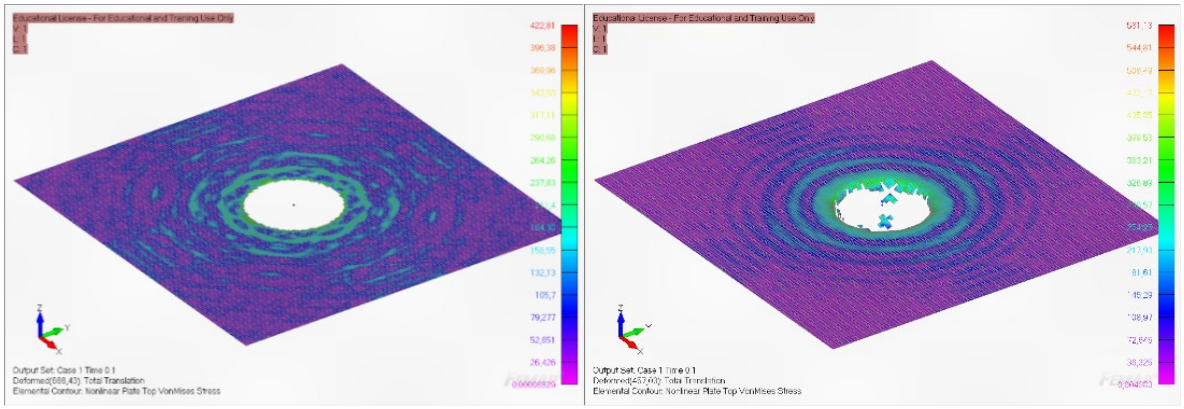

Figure 2.15 Case 12 (left). Case 16 (right). Rigid impactor. Impactor speed v = 5 m/s.

Tabel 2.8. Total impact force. Impactor speed v = 2 m/s.

Case	Impactor type	Elem. Dim. [mm]	μ	Total impact force [MN]
17	Rigid	50	0	2,827
18			0,6	2,827
19		25	0	1,756
20			0,6	1,755
21	Deformable	50	0	1,536
22			0,6	1,536
23		25	0	1,356
24			0,6	1,357

Tabel 2.9. Percentage of affected structure. Impactor speed v = 2 m/s.

Case	Impactor type	Elem. Dim. [mm]	μ	Affected structure %
17	Rigid	50	0	0,13%
18			0,6	0,04%
19		25	0	0,43%
20			0,6	0,45%
21	Deformable	50	0	-
22			0,6	-
23		25	0	0,28%
24			0,6	0,28%

Chapter 3
VALIDATION OF THE THEORETICAL MODELS

3.1 Comparative analysis of methods for estimating ship motions

This section compares two numerical methods used for estimating ship oscillations: the strip method (ST) used in the DYN-OSC program, and the boundary element method (BEM) implemented in Ansys Aqwa. The data obtained through these methods are validated by experimental tests conducted in a towing tank on a scaled-down model for a ship intended for operation in the Caspian Sea.

The experimental tests were conducted on a 1:16 scale model, and measurements were taken for both zero-speed conditions and the towed model at a speed of 1.28 m/s, at different angles of incidence (0°, 90°, 180°). The experimental results were compared with the numerical simulations to evaluate the accuracy and reliability of each method.

The results of the comparative analysis showed good correlation between the numerical methods and the experimental data, although some differences were observed, particularly in the low-frequency ranges, where the experimental data indicated a more amplified response. These discrepancies can be attributed to radiation and diffraction effects present in the physical model, which are not fully captured by the numerical simulations.

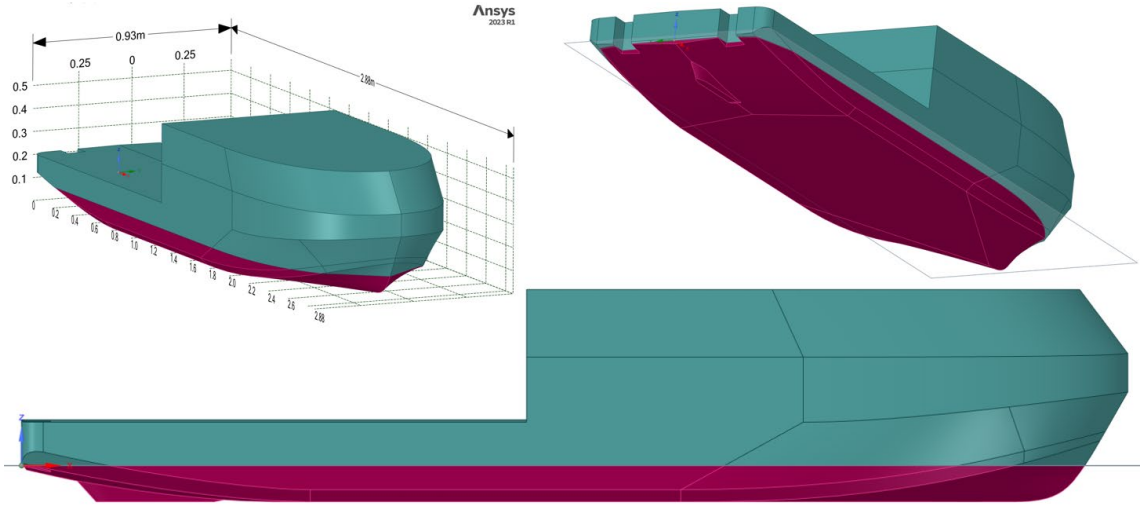

Figure 3.1. CAD geometry. 1:16 scale model. [20], [21]

Figure 3.2. Towing tank ship model. 1:16 scale. [78]

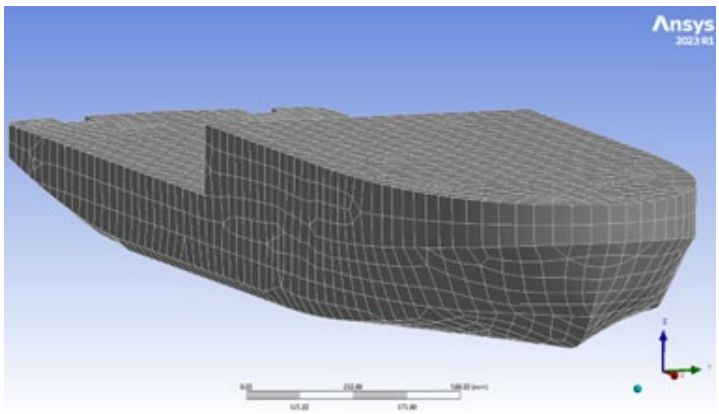

Figure 3.3. Diffraction model discretization. Ansys Aqwa.

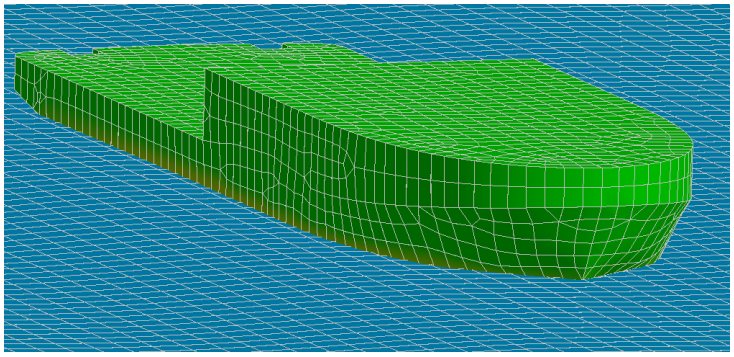

Figure 3.4. Diffraction model discretization and free surface. Ansys Aqwa.

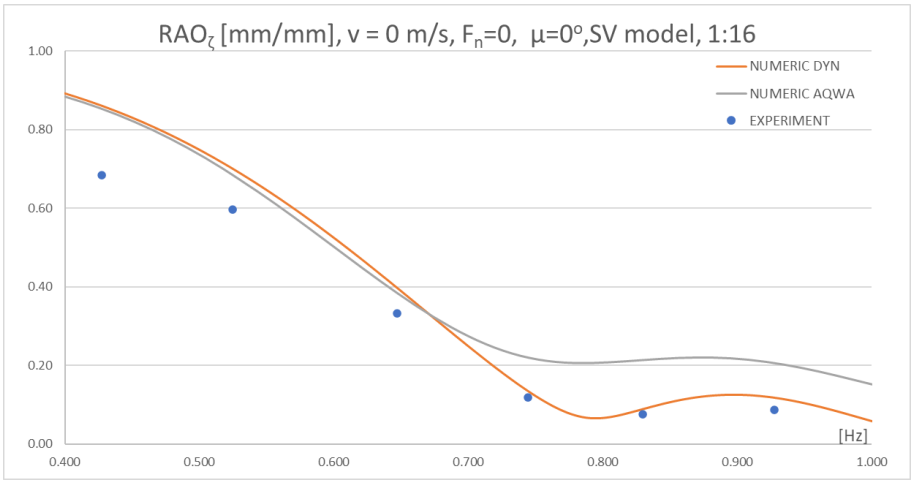

Figure 3.5. Heave motion oscillation (RAOζ), v=0 m/s, μ=0°.

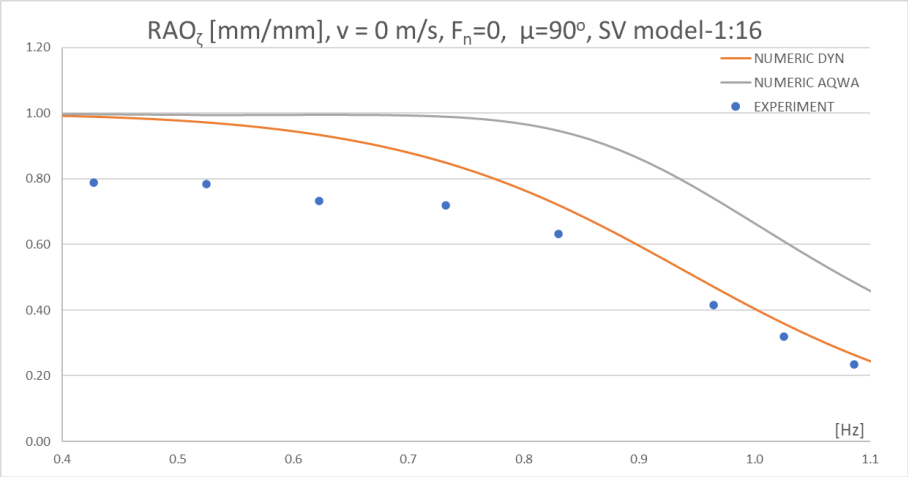

Figure 3.6. Heave motion oscillation (RAOζ), v=0 m/s, μ=90°.

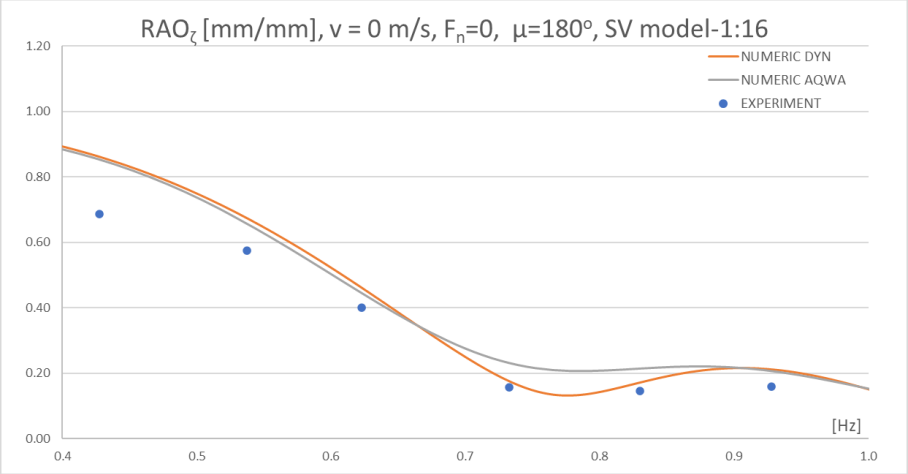

Figure 3.7. Heave motion oscillation (RAOζ), v=0 m/s, μ=180°.

3.2 Validation of the numerical model for bottom impact analysis in case of ship grounding

This section validates the numerical model used for analyzing the structural behavior of a ship in the case of a grounding impact, within the context of grounding. The model was developed using Ansys AutoDyn, and validation was conducted by comparing it with experimental data and benchmarks from the literature.

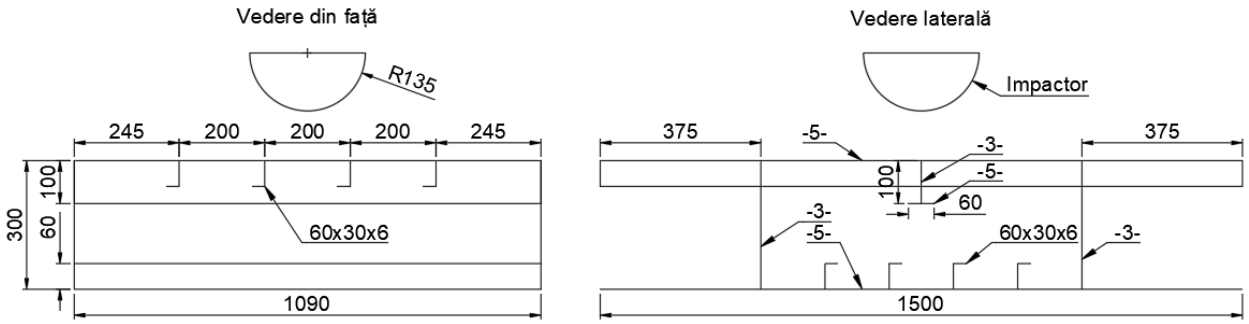

Figure 3.8 Description of the benchmark geometry for grounding impact analysis. [22], [23]

The geometry of the structure used for simulating the grounding impact was taken from a reference study, and the finite elements used in the simulation were meticulously modeled to accurately reproduce real impact conditions. The impact was simulated at a speed of 5 m/s, and the total simulation time was set to allow for complete penetration of the ship's bottom structure.

The simulation results were compared with experimental data, and force-displacement graphs showed good correlation between the simulation and experimental data. The observed differences were minor and were particularly evident in the phase of structural relaxation after the steel plates were fractured. Overall, the results were deemed sufficiently accurate to validate the modeling methodology and confirm the model's ability to correctly assess structural behavior in the case of a grounding impact.

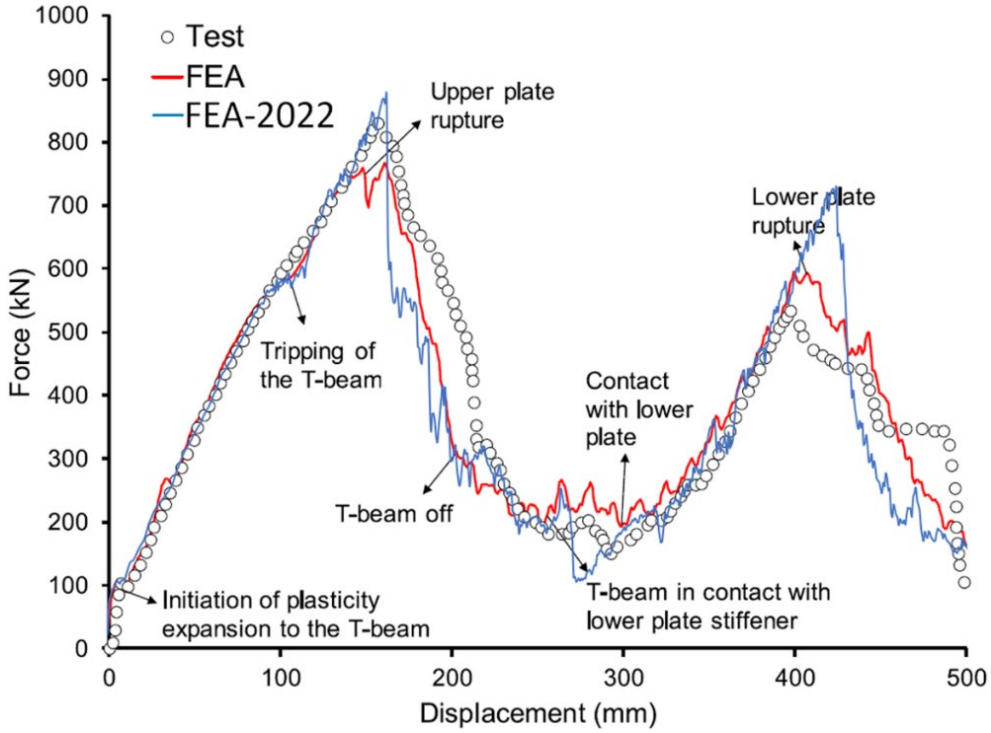

Figure 3.14. Comparison of structural response to grounding impact – experiment / numerical analysis. [22]–[24]

Chapter 4

ANALYSIS OF THE GLOBAL AND LOCAL RESISTANCE USING 1D-3D/FEM MODELS OF A 3000TDW RIVER BARGE

4.1 Preliminary evaluation of the global resistance of a 3000 TDW barge. 1D equivalent beam model

This section presents the preliminary analysis of the structural strength of a 3000 TDW barge using a 1D equivalent beam model. The main goal is to evaluate the bending moments and shear forces on the ship's structure. The simplified 1D model allows for a rapid and efficient analysis of structural stresses, providing an overview of the structural behavior under navigation conditions. In this case, the analyzed barge has the following characteristics: a length of 90 meters, a width of 11 meters, and a displacement of 3620.8 tons when fully loaded.

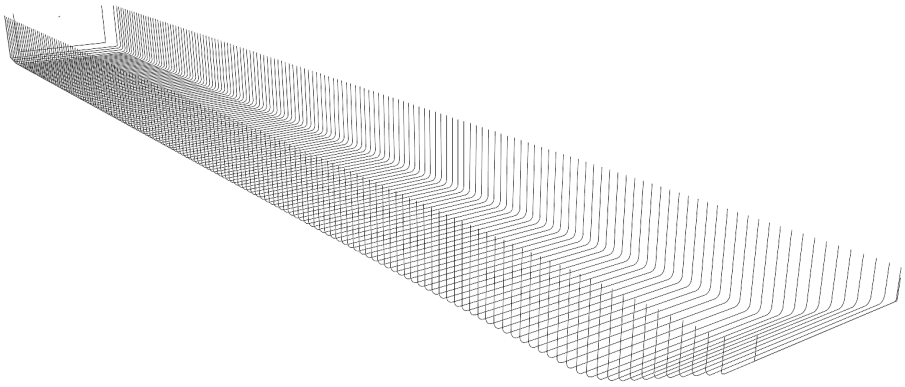

Figure 4.1. Cross-sectional calculation sections, 3000 TDW river barge.

This preliminary assessment is essential for the rapid design of ships, especially used in the initial design stages before applying more complex simulation methods. 1D models are used to calculate sectional stresses, including bending moments and shear forces. These stresses are then transferred to 3D models for detailed analysis.

Tabel 4.1. Main dimensions. 3000 TDW river barge.

Length overall	L_{OA}(m)	90
Breadth	B(m)	11
Depth	D(m)	4.5
Draught	T(m)	3.8
Lightship displacement	D_{light}(t)	507.5
Displacement, Ballast	$D_{ballast}$(t)	529.5
Displacement, full load	D_{FL} (t)	3620.8
Block coefficient	c_b(-)	0.923
Ballast, trim 0°	$M_{ballast}$(t)	22

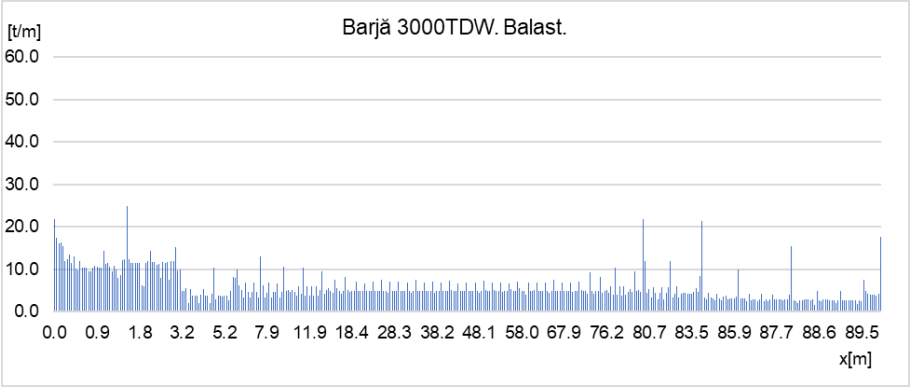

Figure 4.2. Mass distribution along the length. Ballast. 3000 TDW river barge.

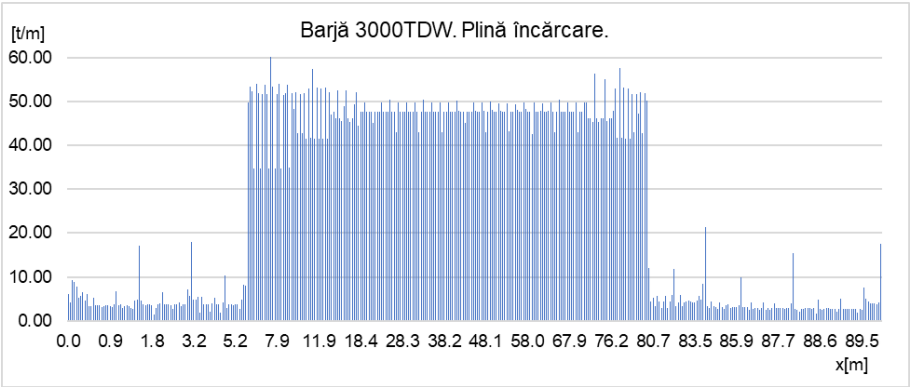

Figura 4.3. Mass distribution along the length. Full load. 3000 TDW river barge.

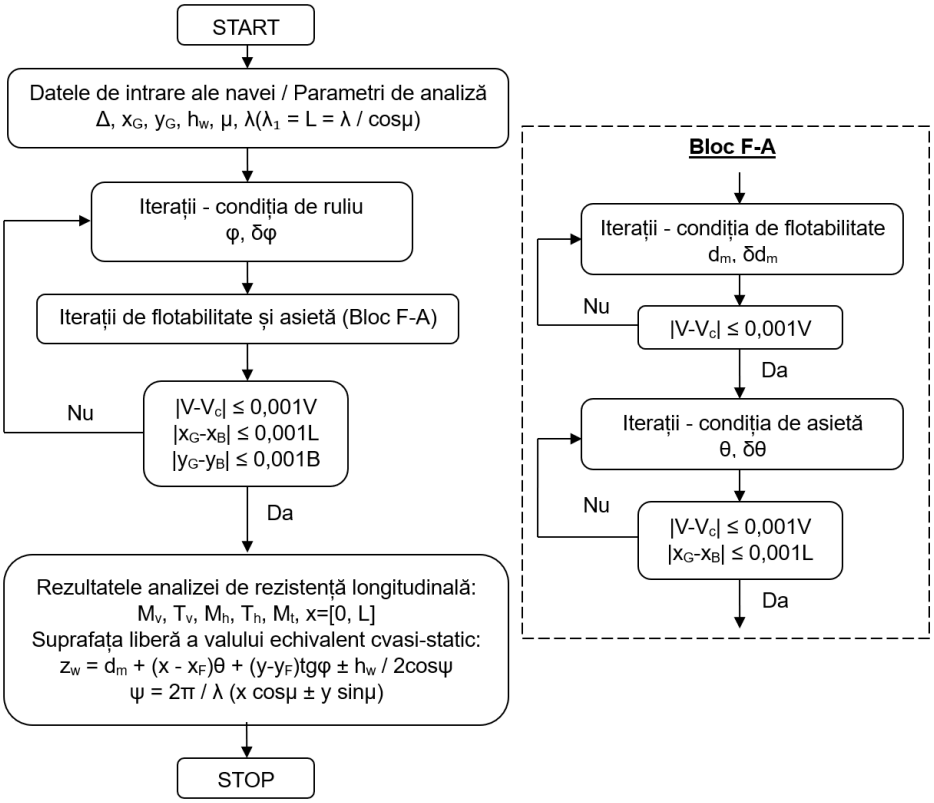

Figure 4.4. Algorithm for balancing a freely floating ship, 1D equivalent beam model.

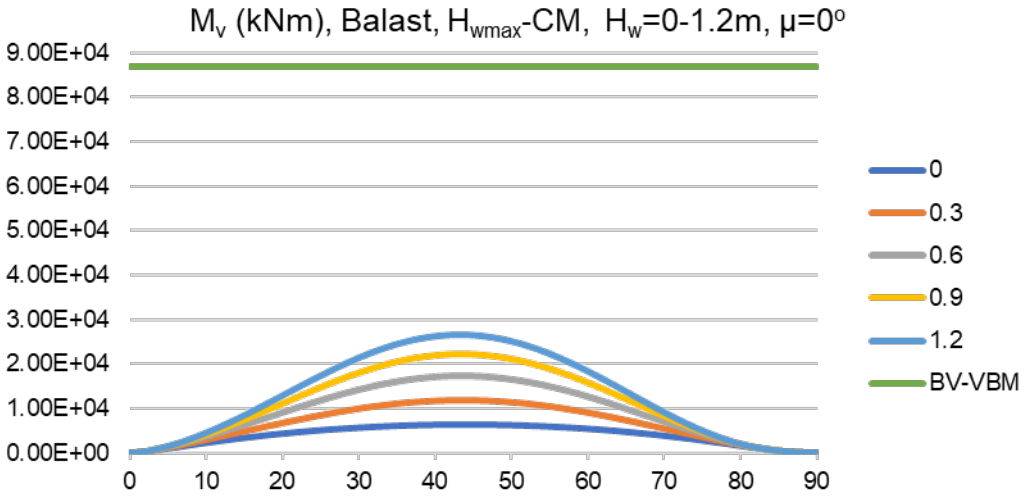

Figure 4.5. Vertical bending moment diagram. Ballast. Hogging wave. μ=0°.

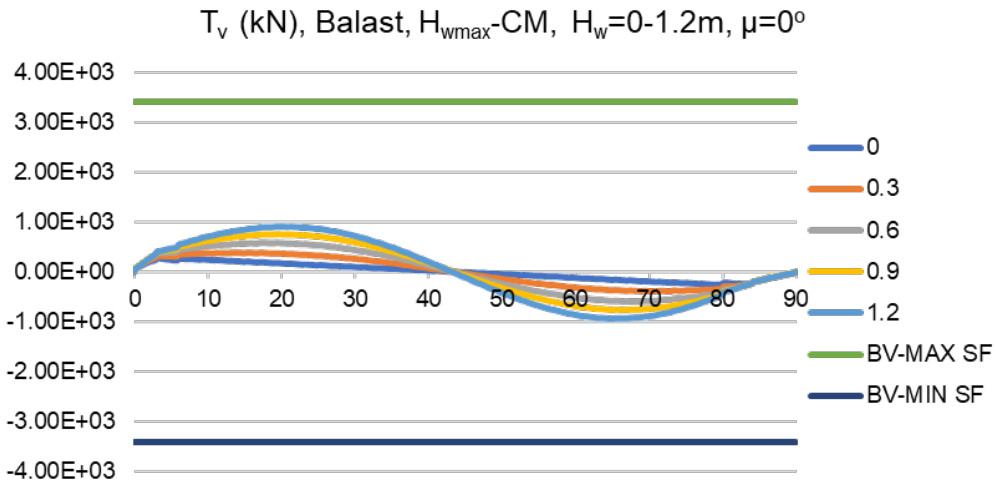

Figure 4.6. Vertical shear force diagram. Ballast. Hogging. μ=0°.

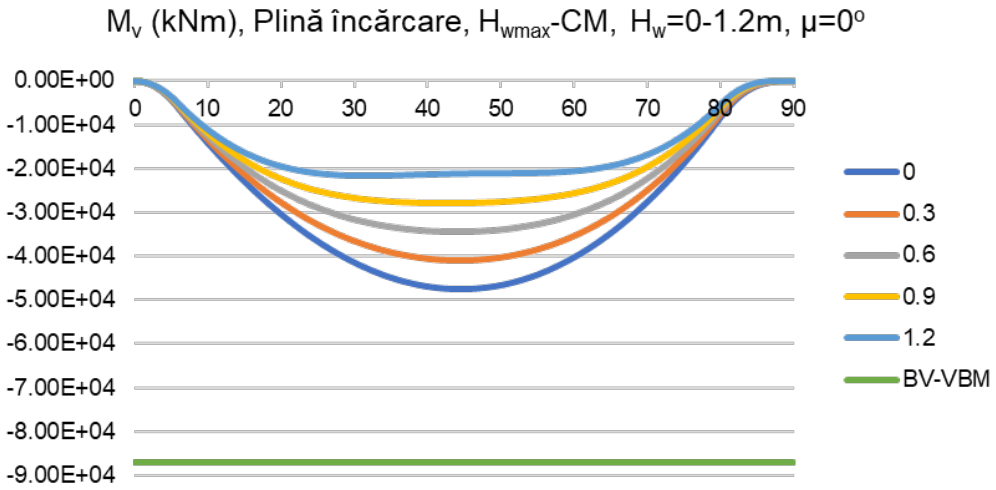

Figure 4.7. Vertical bending moment diagram. Full load. Hogging. μ=0°.

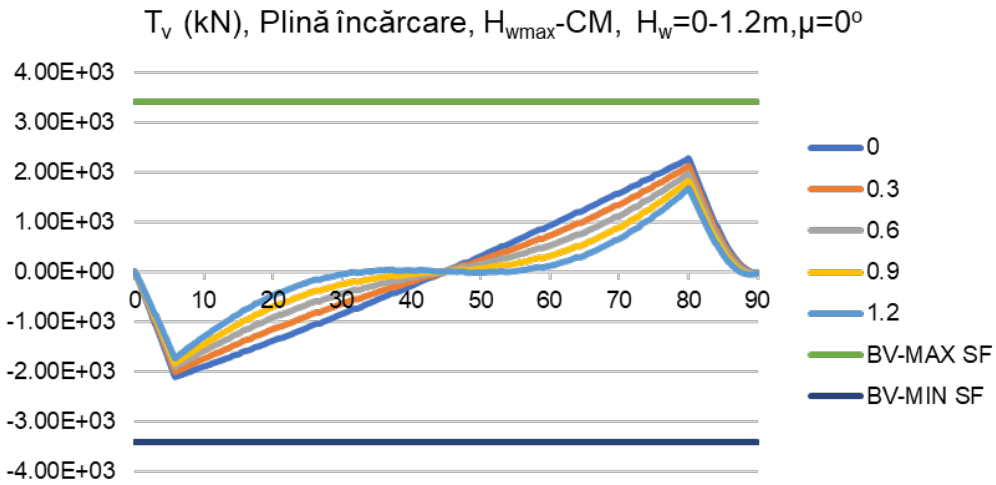

Figure 4.8. Vertical shear force diagram. Full load. Hogging. μ=0°.

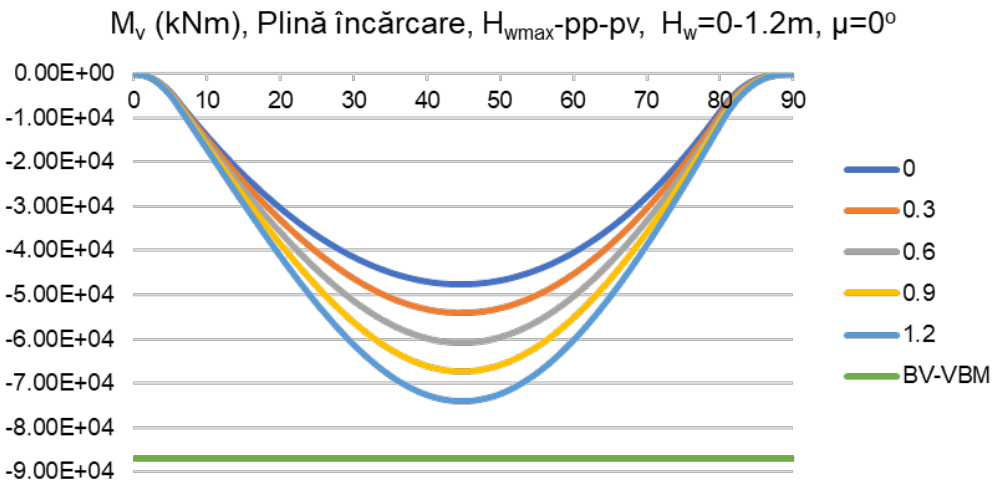

Figure 4.9. Vertical bending moment diagram. Full load. Sagging. μ=0°.

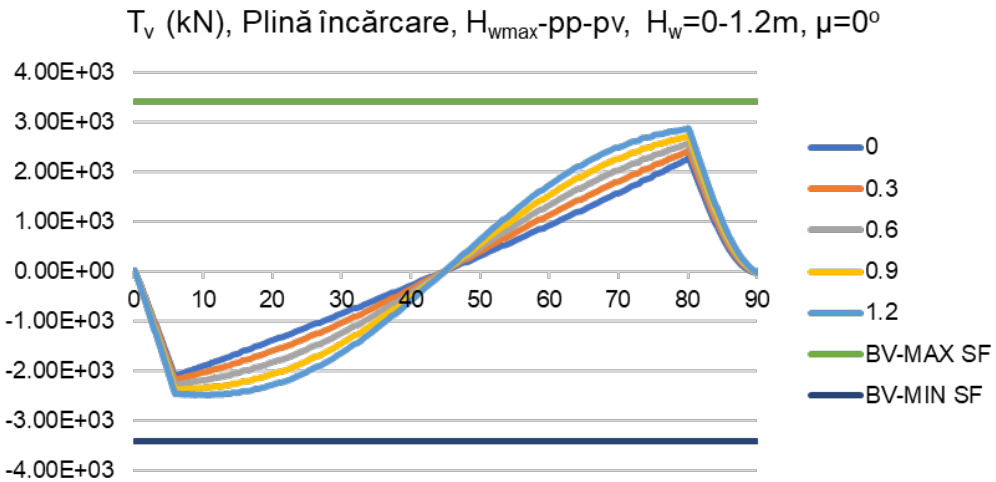

Figure 4.10. Vertical shear force diagram. Full load. Sagging. μ=0°.

4.2 Evaluation of the global and local resistance of a 3000 TDW barge. Extended 3D-FEM model over the entire barge hull

This section extends the analysis by using a complete 3D-FEM model for the 3000 TDW barge. 3D modeling allows for a detailed analysis of stress distribution and structural behavior under complex loads. The model includes structural details such as the deck, ballast tanks, and longitudinal and transverse bulkheads. Two loading scenarios were considered for the structural analysis: ballast and full load.

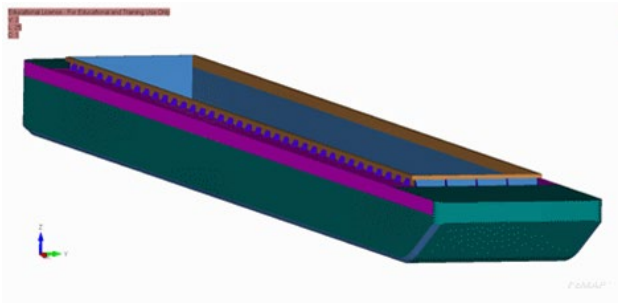

Figure 4.11. 3D-FEM model, 3000 TDW barge.

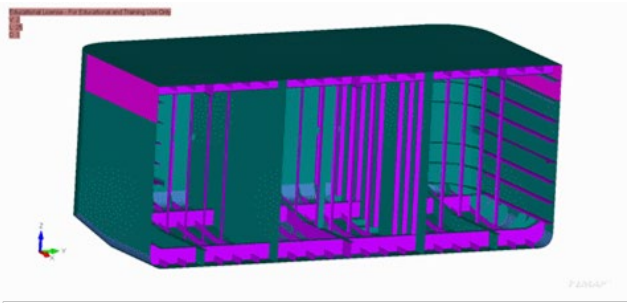

Figure 4.12. Structural detail, aft area, 3000 TDW barge.

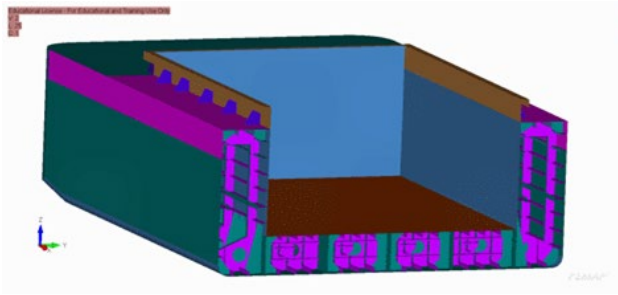

Figure 4.13. Structural detail, aft area of the cargo hold, 3000 TDW barge.

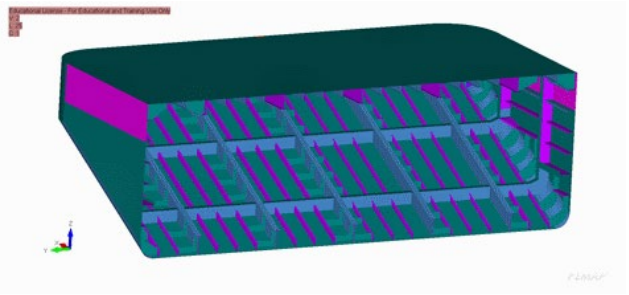

Figure 4.14. Structural detail, bow area, 3000 TDW barge.

4.2.1 Description of the 3D-FEM model and balancing parameters for the 3000 tdw barge – wave conditions

The 3D-FEM model is generated using Siemens Femap NX/Nastran software. The barge geometry is discretized into finite elements, with element sizes ranging from 50 to 75 mm. This model provides a high level of detail and is used to assess stresses and deformations under quasi-static wave actions. The model was balanced under calm water conditions and oblique waves, simulating the impact of waves on the structure.

Tabel 4.3. Boundary conditions for the 3D-FEM model. [25]

Location		Displacement = 0
Aft	Portside	*Z*
	Centerline	*Y*
	Starboard	*Z*
Bow	Centerline	*X, Y, Z*

Tabel 4.4. Equilibrium parameters, 1D model, design equivalent oblique waves, hogging and sagging, 3000 TDW barge, loading case – ballast.

No.	M (°)	Hw (mm)	θ (rad)	φ (rad)	X_F (mm)	Y_F (mm)	T_M (mm)	No.	Θ (rad)	φ (rad)	X_F (mm)	Y_F (mm)	T_M (mm)
LC_1	0	0	0.00001	0	42170.49	0	565.27	-	-	-	-	-	-
LC_2		-300	-0.00076	0	42103.59	0	554.71	LC_26	0.00073	0	42256.59	0	574.92
LC_3		-600	-0.00158	0	42035.69	0	542.65	LC_27	0.00138	0	42259.26	0	583.69
LC_4		-900	-0.00243	0	41967.38	0	528.00	LC_28	0.00198	0	42325.57	0	591.69
LC_5		-1200	-0.00367	0	41895.14	0	505.49	LC_29	0.00253	0	42389.68	0	598.54
LC_6	15	-300	-0.00076	-0.00004	42103.6	0	554.77	LC_30	0.00072	0.00003	42256.57	0	574.87
LC_7		-600	-0.00158	-0.00011	42035.71	0	542.78	LC_31	0.00138	0.00006	42259.24	0	583.60
LC_8		-900	-0.00242	-0.00021	41967.43	-0.01	528.23	LC_32	0.00197	0.00007	42325.53	0	591.57
LC_9		-1200	-0.00366	-0.00081	41895.17	-0.09	505.63	LC_33	0.00252	0.00006	42332.76	0.55	598.24
LC_10	30	-300	-0.00074	-0.00009	42103.65	0	554.98	LC_34	0.00071	0.00007	42256.49	0.01	574.68
LC_11		-600	-0.00155	-0.00023	42035.82	-0.01	543.27	LC_35	0.00135	0.00012	42259.17	0	583.27
LC_12		-900	-0.00238	-0.00045	42003.07	-1.93	528.95	LC_36	0.00194	0.00015	42325.39	0.01	591.10
LC_13		-1200	-0.00365	-0.00177	41895.29	-0.21	506.13	LC_37	0.00248	0.00013	42327.62	0.01	597.61
LC_14	45	-300	-0.00071	-0.00016	42103.77	-0.01	555.52	LC_38	0.00068	0.00012	42256.3	0.01	574.23
LC_15		-600	-0.00147	-0.00039	42099.84	-0.03	544.42	LC_39	0.00129	0.00021	42258.99	0.01	582.41
LC_16		-900	-0.00227	-0.00076	42031.72	-0.08	530.93	LC_40	0.00186	0.00026	42325.02	0.01	589.92
LC_17		-1200	-0.00361	-0.00306	41895.61	-0.35	507.47	LC_41	0.00238	0.00023	42327.23	0.01	596.06
LC_18	60	-300	-0.00059	-0.00026	42112.68	-0.91	557.08	LC_42	0.00058	0.0002	42255.68	0.02	572.88
LC_19		-600	-0.00125	-0.00062	42101.24	-0.04	548.02	LC_43	0.00111	0.00035	42258.44	0.02	579.91
LC_20		-900	-0.00194	-0.00118	42034.3	-0.06	537.11	LC_44	0.0016	0.00046	42323.89	0.03	586.39
LC_21		-1200	-0.00343	-0.00481	41913.22	-1.99	512.42	LC_45	0.00208	0.00027	42326.01	0.02	593.59
LC_22	75	-300	-0.00009	-0.00041	42170.17	-0.02	564.25	LC_46	0.00012	0.00036	42170.84	0.02	566.46
LC_23		-600	-0.00023	-0.001	42169.81	-0.05	564.63	LC_47	0.00021	0.00070	42171.15	0.03	567.52
LC_24		-900	-0.00042	-0.00162	42168.97	-0.12	565.74	LC_48	0.0003	0.00103	42173.89	0.29	568.29
LC_25		-1200	-0.00074	-0.00278	42142.98	-0.18	566.37	LC_49	0.00049	0.00004	42237.6	0	591.18

4.2.2 Global-local resistance, 3D-FEM model for the 3000 tdw barge, in ballast navigation

The ballast navigation case analysis includes 49 loading scenarios, simulating oblique waves with heights ranging from 0 to 1.2 meters. The evaluation results indicated that maximum stresses occur at the transition between the cargo hold and the ballast tanks in the aft and bow areas. For waves with a height of 1.2 meters, the equivalent von Mises stresses reached 59.96 MPa, and the maximum vertical deformations were 68 mm.

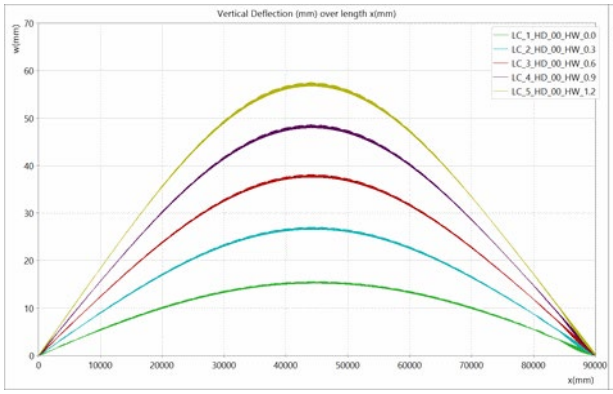

Figure 4.15. Vertical deformation (mm) along length x (mm), μ=0°, Ballast loading case, bending moment in hogging, 3000 TDW barge.

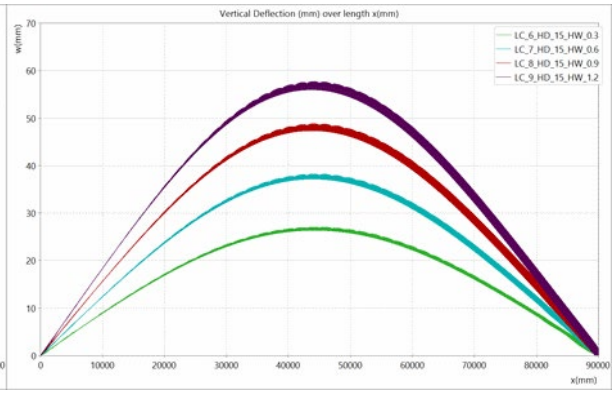

Figure 4.16. Vertical deformation (mm) along length x (mm), μ=15°, Ballast loading case, bending moment in hogging, 3000 TDW barge.

Tabel 4.6. Results of the 3D-FEM analysis of global-local strength, 3000 TDW barge, hogging and sagging, ballast loading condition.

Nr.	*μ* (°)	*Hw* (mm)	σ_{VM} (Mpa)	w_{max} (mm)	*YR* -	*DR* -	*Nr.*	σ_{VM} (Mpa)	w_{max} (mm)	*YR* -	*DR* -
LC_1	0	0	19.00	15.64	0.095	0.087	-	-	-	-	-
LC_2		300	25.57	27.13	0.128	0.151	LC_26	18.54	4.051	0.093	0.023
LC_3		600	35.56	38.24	0.178	0.212	LC_27	17.80	8.213	0.089	0.046
LC_4		900	46.23	48.75	0.231	0.271	LC_28	22.67	20.229	0.114	0.112
LC_5		1200	55.52	57.66	0.278	0.320	LC_29	34.75	32.372	0.174	0.180
LC_6	15	300	25.57	27.17	0.128	0.151	LC_30	18.55	4.165	0.093	0.023
LC_7		600	35.62	38.37	0.178	0.213	LC_31	17.99	8.532	0.090	0.047
LC_8		900	46.32	48.98	0.232	0.272	LC_32	22.76	20.710	0.114	0.115
LC_9		1200	55.58	57.89	0.278	0.322	LC_33	34.86	32.998	0.175	0.183
LC_10	30	300	25.55	27.26	0.128	0.151	LC_34	18.56	4.435	0.093	0.025
LC_11		600	35.65	38.59	0.178	0.214	LC_35	17.94	8.895	0.090	0.049
LC_12		900	46.38	49.43	0.232	0.275	LC_36	22.76	21.214	0.114	0.118
LC_13		1200	55.51	58.33	0.278	0.324	LC_37	34.86	33.647	0.175	0.187
LC_14	45	300	25.48	27.39	0.128	0.152	LC_38	18.41	4.917	0.092	0.027
LC_15		600	35.62	39.09	0.178	0.217	LC_39	17.66	9.361	0.088	0.052
LC_16		900	46.36	50.25	0.232	0.279	LC_40	22.58	21.820	0.113	0.121
LC_17		1200	55.18	59.04	0.276	0.328	LC_41	34.58	34.389	0.173	0.191
LC_18	60	300	25.28	27.69	0.127	0.154	LC_42	17.69	5.832	0.089	0.032
LC_19		600	35.35	39.91	0.177	0.222	LC_43	18.73	10.072	0.094	0.056
LC_20		900	46.12	51.80	0.231	0.288	LC_44	21.78	22.672	0.109	0.126
LC_21		1200	54.19	60.18	0.271	0.334	LC_45	32.94	**34.640**	0.165	**0.192**
LC_22	75	300	26.83	27.78	0.134	0.154	LC_46	19.55	8.386	0.098	0.047
LC_23		600	36.84	40.95	0.184	0.228	LC_47	23.67	11.740	0.119	0.065
LC_24		900	48.58	54.42	0.243	0.302	LC_48	27.79	23.820	0.139	0.132
LC_25		1200	**59.96**	**68.06**	**0.300**	**0.378**	LC_49	**35.18**	29.323	**0.176**	0.163

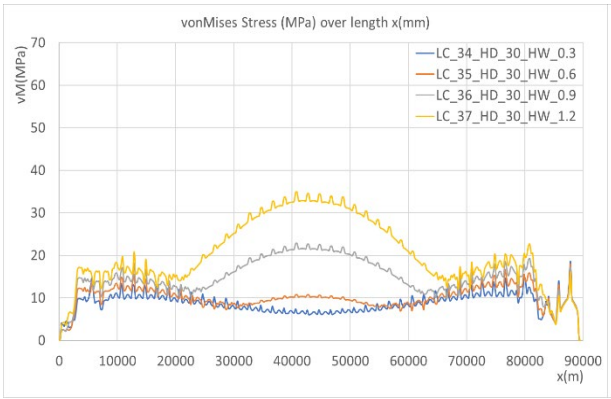

Figure 4.17. Von Mises stresses (MPa) along length x (mm), μ=30°, Ballast loading case, bending moment in sagging, 3000 TDW barge.

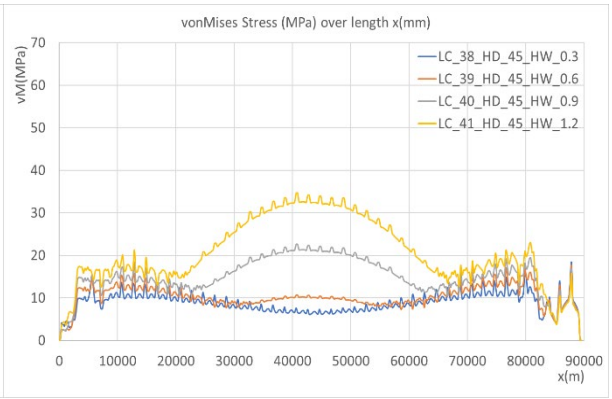

Figure 4.18. Von Mises stresses (MPa) along length x (mm), μ=45°, loading condition - ballast, bending stress in sagging, 3000 TDW barge.

4.2.3 Global-local resistance, 3D-FEM model for the 3000 tdw barge, in full-load navigation

This section analyzes the full-load scenarios of the barge, including 49 cases of hogging and sagging stresses. As with the ballast condition, oblique waves with varying heights were considered. The maximum von Mises stresses were 158.18 MPa, and the maximum vertical deformations reached 177.07 mm under the most severe loading conditions.

The results obtained from the 1D and 3D-FEM models show that stresses and deformations are significantly influenced by wave height and loading scenarios. In the case of full-load navigation, the maximum stresses are close to the allowable limit, highlighting the importance of correctly designing the barge's structure to withstand extreme operational conditions.

Tabel 4.7. Rezultatele analizei 3D-FEM a rezistenței globale-locale, barja 3000 tdw, crestă și gol de val, condiția de plină încărcare.

No.	μ (°)	Hw (mm)	σ_{VM} (Mpa)	w (mm)	YR -	DR -	Nr.	σ_{VM} (Mpa)	w (mm)	YR -	DR -
-		-	-	-	-	-	LC_74	123.80	118.49	0.620	0.658
LC_50		300	151.20	103.900	0.757	0.577	LC_75	130.43	133.12	0.653	0.740
LC_51	0	600	135.32	89.317	0.677	0.496	LC_76	137.03	147.76	0.686	0.821
LC_52		900	132.77	74.752	0.665	0.415	LC_77	147.37	162.43	0.738	0.902
LC_53		1200	142.76	60.297	0.715	0.335	LC_78	**158.18**	177.07	**0.792**	0.984
LC_54		300	151.20	103.970	0.757	0.578	LC_79	130.57	133.14	0.654	0.740
LC_55	15	600	135.32	89.455	0.677	0.497	LC_80	137.32	147.8	0.687	0.821
LC_56		900	132.65	74.957	0.664	0.416	LC_81	147.36	162.48	0.738	0.903
LC_57		1200	142.60	60.569	0.714	0.336	LC_82	**158.18**	**177.14**	**0.792**	0.984
LC_58		300	151.22	104.120	0.757	0.578	LC_83	130.64	133.11	0.654	0.740
LC_59	30	600	135.36	89.752	0.678	0.499	LC_84	137.46	147.74	0.688	0.821
LC_60		900	132.09	75.400	0.661	0.419	LC_85	147.32	162.39	0.738	0.902
LC_61		1200	141.85	61.156	0.710	0.340	LC_86	158.13	177.03	0.792	0.984
LC_62		300	151.27	104.420	0.757	0.580	LC_87	130.59	132.96	0.654	0.739
LC_63	45	600	135.48	90.371	0.678	0.502	LC_88	137.36	147.45	0.688	0.819
LC_64		900	131.34	76.328	0.658	0.424	LC_89	147.20	161.95	0.737	0.900
LC_65		1200	140.63	62.366	0.704	0.346	LC_90	157.98	176.47	0.791	0.980
LC_66		300	151.46	105.230	0.758	0.585	LC_91	130.08	132.43	0.651	0.736
LC_67	60	600	135.83	91.991	0.680	0.511	LC_92	136.34	146.38	0.683	0.813
LC_68		900	130.22	78.766	0.652	0.438	LC_93	146.82	160.35	0.735	0.891
LC_69		1200	139.15	65.538	0.697	0.364	LC_94	157.45	174.33	0.788	0.969
LC_70		300	**152.47**	**108.950**	**0.763**	**0.605**	LC_95	126.48	129.44	0.633	0.719
LC_71	75	600	137.80	99.416	0.690	0.552	LC_96	134.73	140.41	0.674	0.780
LC_72		900	126.11	90.492	0.631	0.503	LC_97	144.61	151.63	0.724	0.842
LC_73		1200	132.77	81.725	0.665	0.454	LC_98	154.49	163.33	0.773	0.907

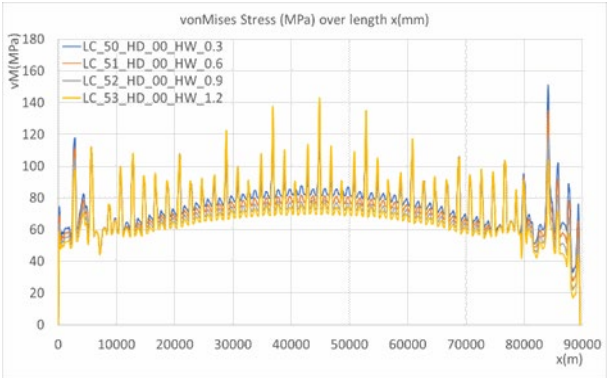

Figure 4.19. Von Mises Stresses (MPa) along Length x (mm), μ=0°, Full Load Case, Hogging Stress, 3000 TDW Barge

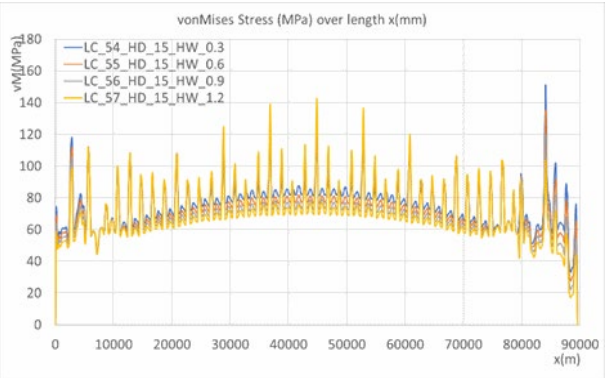

Figure 4.20. Von Mises Stresses (MPa) along Length x (mm), μ=15°, Full Load Case, Hogging Stress, 3000 TDW Barge

Chapter 5

COMPARATIVE ANALYSIS OF THE STRUCTURAL PERFORMANCE OF A RIVER-COASTAL VESSEL BUILT FROM COMPOSITE MATERIAL

5.1 Use of composite materials in shipbuilding

Composite materials, particularly glass-reinforced epoxy resin (GRE), have become increasingly utilized in shipbuilding due to their significant advantages: reduced weight, superior mechanical strength, and structural efficiency. These materials offer durable solutions for vessels, especially in terms of reducing maintenance costs and enhancing performance. This chapter focuses on a 24-meter river-coastal vessel constructed from GRE and examines how the material influences its structural behavior.

5.2 Constructive and mechanical characteristics of the composite material

GRE composite materials are preferred for small sized ships due to their high mechanical properties, such as tensile strength and elastic modulus, which contribute to the rigidity and strength of the structure. This section describes experimental tests conducted on different types of composite materials, highlighting the behavioral differences between them. Two composite variants were analyzed: a simplified one without an intermediate layer (A1) and a complex one (A2) with additional layers for structural reinforcement. The results show that material A2 exhibits greater rigidity and superior mechanical strength compared to A1.

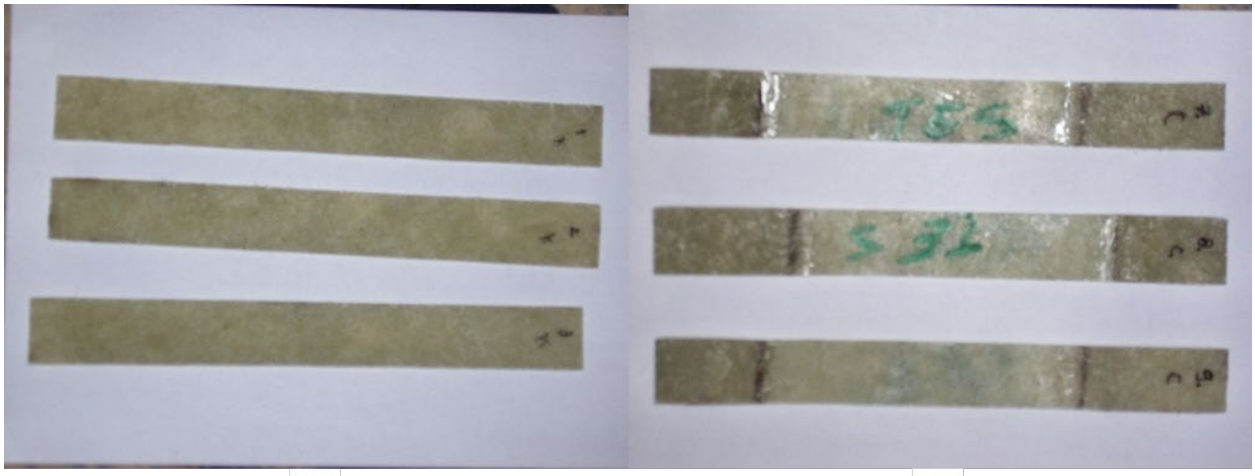

a b

Figure 5.1. Composite specimens GRE, A1 and A2.

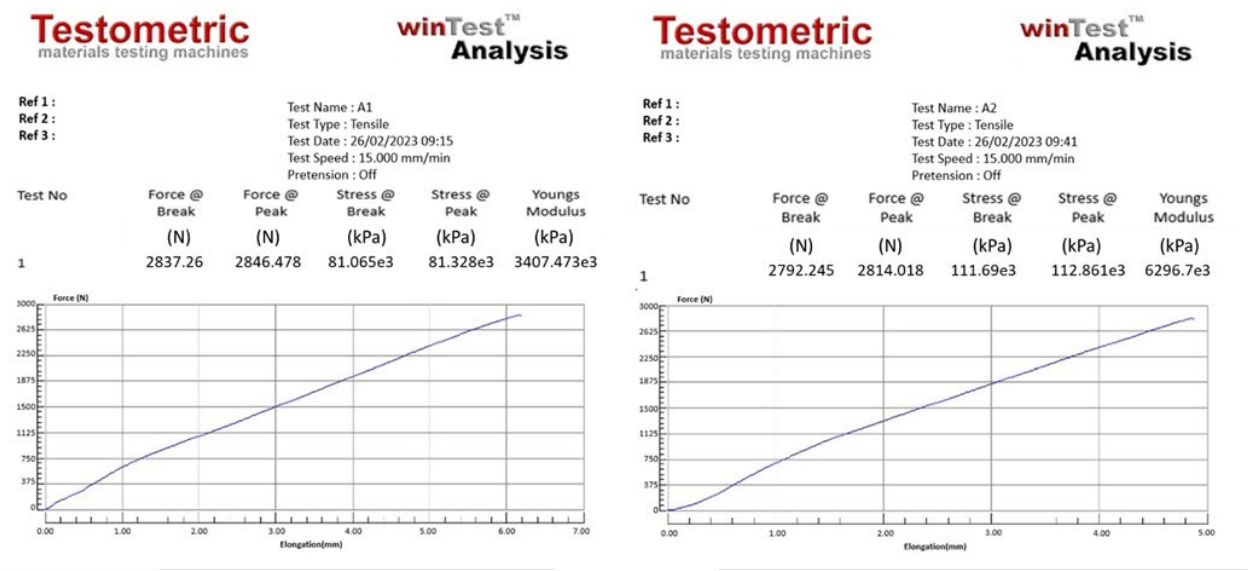

Figure 5.2. Tensile force-extension curves for composite specimens GRE types A1 and A2.

Tabel 5.1. Characteristics of composite materials GRE A1 and A2

Material	L x l x t			Break Force	R_m	E	v	ρ_m	von Mises adm.	Buckling factor adm.	Max. vert. deflection adm.
	[mm]			[N]	[kPa]	[kPa]	[-]	[kg/m^3]	[kPa]	[-]	[mm]
A1	200	10	3.5	2837	8.11E+04	3.41E+06	0.275	1320	20.27E+03	1.3	+/-85
A2	200	10	2.5	2962	1.12E+05	6.30E+06	0.275		27.92E+03		

5.3 Structural model with finite elements for the river-coastal vessel

This section presents the structural modeling of the river-coastal vessel using the finite element method (FEM). The created model includes all the structural details of the vessel, such as the decks, side and longitudinal walls, as well as the hull geometry. This approach allows for the simulation of the vessel's structural behavior under various loading conditions and wave scenarios. The model is used to evaluate equivalent stresses and deformations, providing a clear picture of how composite materials influence the overall structural performance of the vessel.

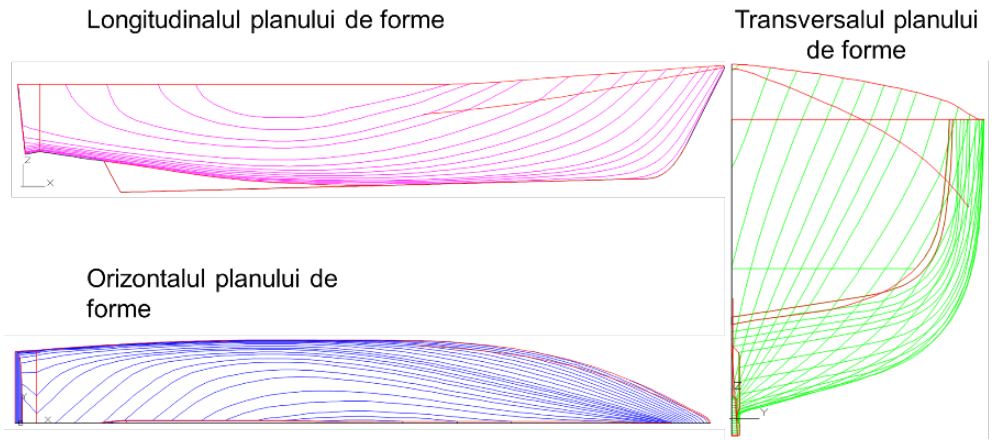

Figure 5.3. Lines body plan, GRE-RC Boat

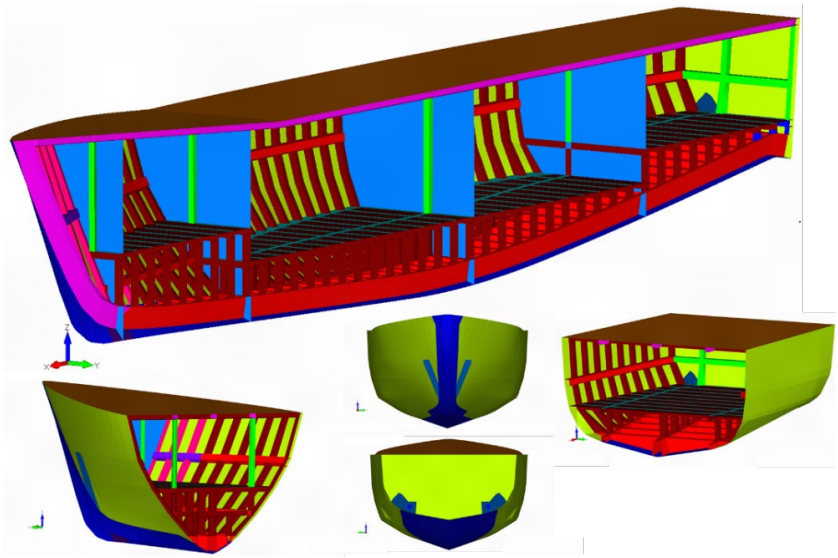

Figure 5.4. 3D-FEM model of the river-coastal vessel made of composite materials.

5.4 Balancing parameters of the river-coastal vessel made from GRE in designed oblique wave conditions

This section analyzes the behavior of the vessel in oblique waves, using simulations for different wave heights and angles of attack. The results show that wave height and angle of attack have a significant impact on the stability and structural integrity of the vessel. The simulated models were balanced to reflect real operating conditions, and the results were compared with the safety criteria imposed by classification societies. It was observed that material A2 provides better stability in high wave conditions, while A1 tends to exceed permissible limits under certain extreme conditions.

Tabel 5.5. Equilibrium parameters for ship-wave interaction. River-coastal vessel made of GRE composite materials. Wave crest at the midship section (hogging).

Param. 1D Model	*μ[°]*	0	*Wave height h_w [m]*									
			0.5	*1*	*1.5*	*2*	*2.5*	*3*	*3.5*	*4*	*4.5*	*5*
Draught (m)	0	1.5	1.440	1.360	1.250	1.112	0.933	0.744	0.501	0.442	0.229	0.058
	15		1.441	1.362	1.255	1.119	0.939	0.758	0.524	0.445	0.235	0.061
	30		1.445	1.372	1.271	1.143	0.960	0.808	0.634	0.439	0.279	0.103
	45		1.454	1.394	1.311	1.151	1.014	0.906	0.716	0.573	0.384	0.186
	60		1.479	1.437	1.373	1.285	1.194	1.065	0.948	0.827	0.664	0.566
	75		1.548	1.521	1.396	1.354	1.291	1.229	1.129	1.090	0.845	0.805
Trim (rad)	0	0.0	-0.017	-0.034	-0.051	-0.070	-0.002	-0.112	-0.134	-0.003	-0.003	-0.003
	15		-0.017	-0.034	-0.051	-0.070	-0.002	-0.112	-0.134	-0.003	-0.003	-0.003
	30		-0.016	-0.033	-0.050	-0.069	-0.002	-0.111	-0.002	-0.003	-0.002	-0.003
	45		-0.015	-0.031	-0.048	-0.002	-0.002	-0.103	-0.002	-0.002	-0.002	-0.002
	60		-0.011	-0.001	-0.001	-0.001	-0.001	-0.001	-0.001	0.000	-0.001	0.000
	75		0.008	0.014	0.000	0.000	-0.001	-0.013	-0.006	0.000	0.070	0.070
Heel (rad)	0	0.0	0.000	0.000	0.000	0.000	0.000	0.000	0.000	0.000	0.000	0.000
	15		-0.007	-0.015	-0.022	-0.028	-0.010	-0.042	-0.048	-0.014	-0.014	-0.016
	30		-0.016	-0.031	-0.046	-0.061	-0.033	-0.089	-0.040	-0.042	-0.045	-0.044
	45		-0.025	-0.051	-0.077	-0.058	-0.065	-0.127	-0.073	-0.079	-0.077	-0.082
	60		-0.037	-0.058	-0.082	-0.099	-0.112	-0.117	-0.122	-0.117	-0.115	-0.120
	75		-0.018	-0.036	-0.060	-0.131	-0.094	-0.122	-0.094	-0.133	0.031	0.051

Tabel 5.6. Ship-wave equilibrium parameters. River-coastal craft made of GRE composite materials. Wave crest stern-bow (sagging).

Param. 1D Model	*μ[°]*	0	*Wave height h_w [m]*									
			0.5	1	1.5	2	2.5	3	3.5	4	4.5	5
Draught (m)	0	1.5	1.546	1.581	1.608	1.626	1.630	1.617	1.580	1.524	1.463	1.410
	15		1.545	1.580	1.606	1.622	1.627	1.614	1.590	1.509	1.444	1.390
	30		1.542	1.574	1.597	1.612	1.615	1.601	1.555	1.454	1.352	1.326
	45		1.534	1.559	1.575	1.584	1.582	1.563	1.519	1.425	1.342	1.317
	60		1.513	1.517	1.514	1.503	1.484	1.498	1.286	1.254	1.154	1.119
	75		1.443	1.357	1.383	1.159	1.240	1.349	1.262	1.223	1.120	1.108
Trim (rad)	0	0.0	0.015	0.030	0.042	0.053	0.063	0.071	0.075	0.083	0.092	0.102
	15		0.015	0.029	0.041	0.052	0.061	0.069	0.077	0.082	0.090	0.100
	30		0.014	0.027	0.038	0.047	0.052	0.061	0.063	0.077	0.086	0.092
	45		0.012	0.022	0.030	0.036	0.036	0.043	0.039	0.048	0.052	0.057
	60		0.006	0.009	0.009	0.000	0.000	-0.001	0.022	0.038	0.049	0.055
	75		-0.012	-0.002	-0.001	-0.001	-0.001	0.000	-0.001	0.000	0.000	0.000
Heel (rad)	0	0.0	0.000	0.000	0.000	0.000	0.000	0.000	0.000	0.000	0.000	0.000
	15		0.007	0.014	0.021	0.029	0.036	0.036	0.037	0.040	0.047	0.048
	30		0.015	0.030	0.045	0.060	0.068	0.091	0.094	0.101	0.110	0.119
	45		0.024	0.048	0.073	0.089	0.117	0.138	0.172	0.157	0.157	0.174
	60		0.035	0.069	0.096	0.136	0.175	0.205	0.192	0.188	0.185	0.181
	75		0.015	0.005	0.106	0.038	0.040	0.066	0.056	0.047	0.045	0.041

5.5 Structural analysis of the river-coastal vessel - first constructive version

The first version of the vessel's structure is analyzed in detail under different loading scenarios. FEM analyses show that composite material A1 exhibits higher von Mises stresses than A2, and in the case of waves exceeding 4 meters and large attack angles, the stresses surpass safety limits. Vertical deformations are also significantly higher for A1, indicating that this material does not provide sufficient rigidity for the designed operating conditions.

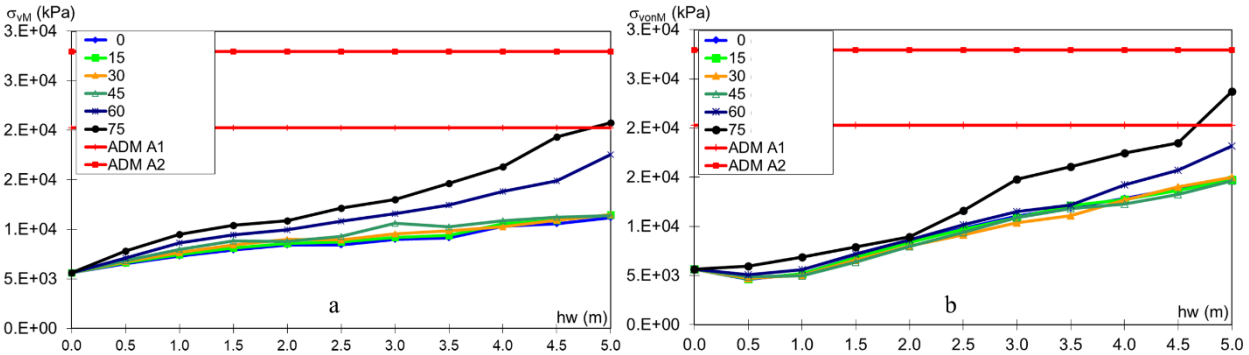

Figure 5.5. Material A1-A2. Von Mises stresses, hogging (a) and sagging (b). Group T. 1.

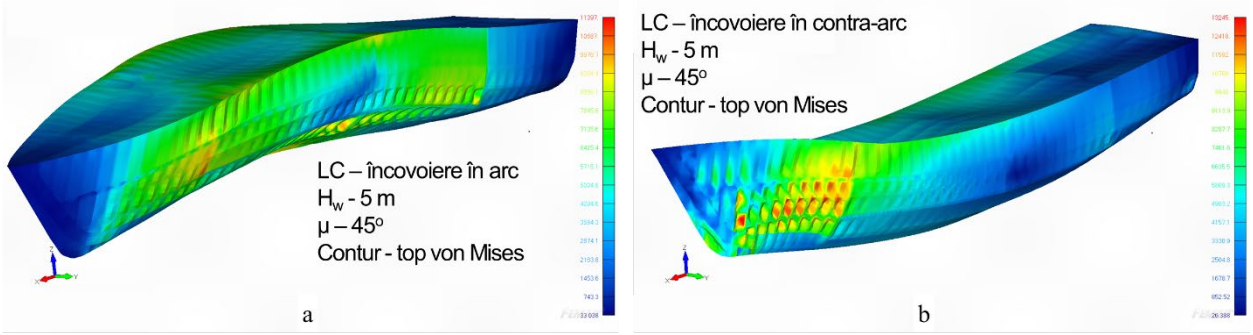

Figure 5.6. Material A1-A2. Von Mises stresses, hogging (a) and sagging (b). Group T. 1.

5.6 Structural analysis of the river-coastal vessel - second constructive version

The second version of the vessel, constructed with material A2 and additional thickness for the main structures, shows a significant improvement in structural behavior. The von Mises stresses and vertical deformations remain within allowable limits for all simulated operating conditions. This version was able to withstand waves up to 5 meters without exceeding the safety criteria established by international regulations.

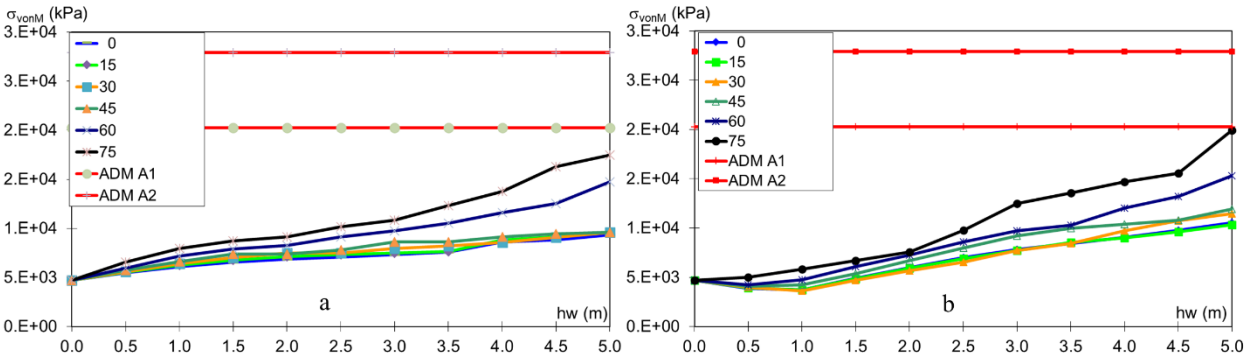

Figure 5.7. Material A1-A2. Von Mises stresses, hogging (a) and sagging (b). Group T. 2.

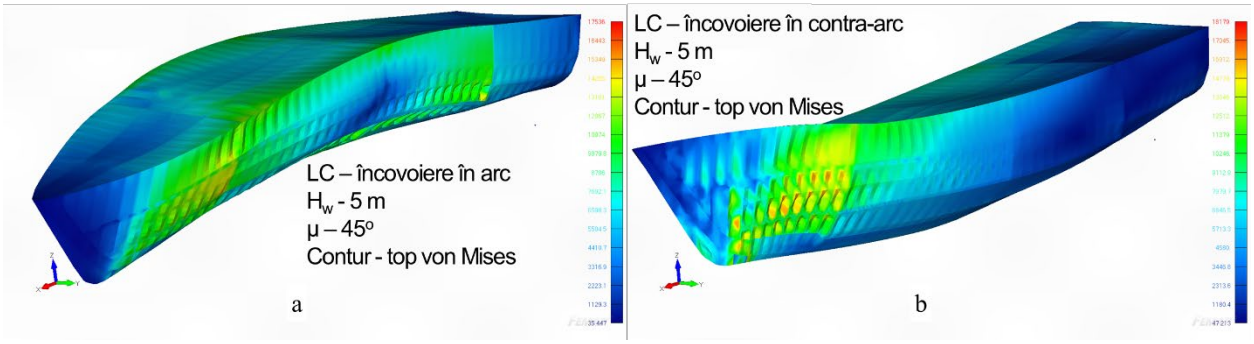

Figure 5.8. Material A1-A2. Von Mises stresses, hogging (a) and sagging (b). Group T. 2.

5.7 Structural analysis of the river-coastal vessel - third constructive version

The third version of the vessel's structure, with additional thickness in critical areas, presents the best results. Analyses show that both von Mises stresses and vertical deformations are well below allowable limits, even under extreme wave and loading conditions. This version optimizes structural performance, ensuring an ideal balance between strength and weight.

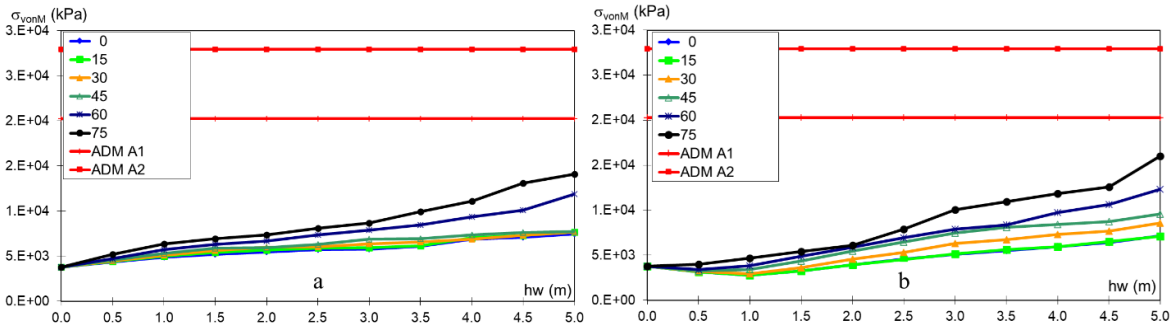

Figure 5.9. Material A1-A2. Von Mises stresses, hogging (a) and sagging (b). Group T. 3.

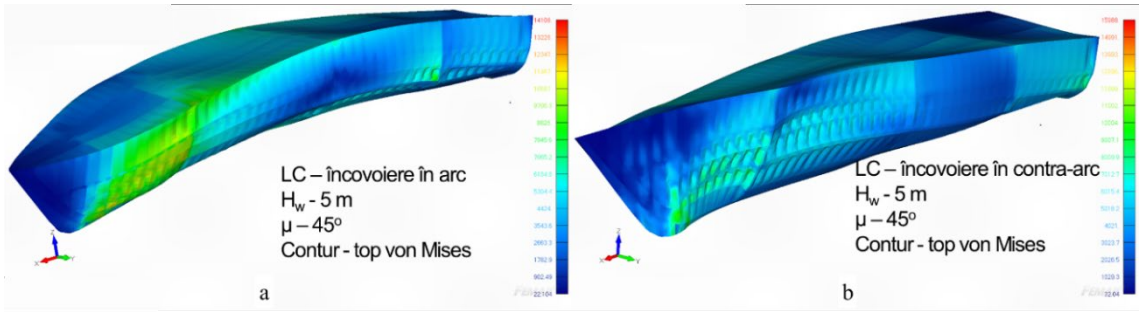

Figure 5.10. Material A1-A2. Von Mises stresses, hogging (a) and sagging (b). Group T. 3.

5.8 Conclusions on the comparative analysis of the river-coastal vessel structure made of GRE composite materials

The comparative analysis showed that composite material A2, combined with the appropriate thicknesses from versions T2 and T3, provides the best structural performance for the river-coastal vessel. Material A1, although lighter, failed to meet safety criteria under certain operating conditions. In conclusion, the use of material A2, along with additional thicknesses, is recommended to ensure the vessel's safety and durability in challenging operating conditions.

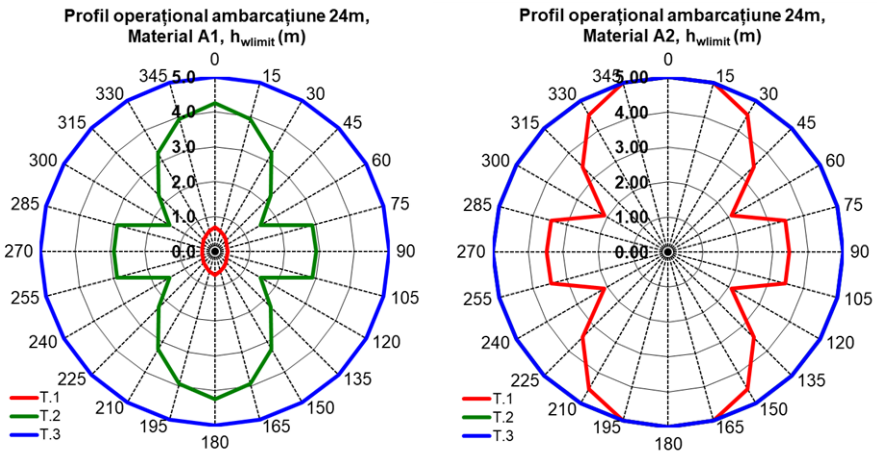

Figure 5.11. Operational profile, GRE composite materials A1, A2, based on local-global structural strength criteria.

Chapter 6

ANALYSIS OF THE DYNAMIC BEHAVIOR OF A 3000 TDW BARGE IN WAVES

6.1 Comparative analysis of the 3000 tdw barge dynamics using 2D-3D methods

In this section, a comparative analysis of the dynamic behavior of the 3000 TDW barge was conducted using two numerical methods: the strip method (2D) and the boundary element method (3D). Both methods had been previously validated, and the main objective was to compare the responses in terms of vertical heave, roll, and pitch oscillations. Tests were performed under both zero-speed conditions and at a speed of 15 km/h to assess the impact of speed on the vessel's dynamics. The results showed significant differences between the two methods, particularly at higher speeds, where the 3D model demonstrated greater sensitivity in handling complex hydrodynamic interactions.

6.1.1 Vertical translation oscillation

The results for vertical heave oscillations show good correspondence between the two methods at low frequencies, but at higher speeds and frequencies, the 3D model exhibits slightly larger amplitudes. This suggests that the 3D method is more sensitive to complex dynamic effects, particularly in the resonance range, where hydrodynamic interactions are more pronounced. At a speed of 15 km/h, the differences become more significant, indicating a tendency for the 3D model to present larger responses compared to the 2D model.

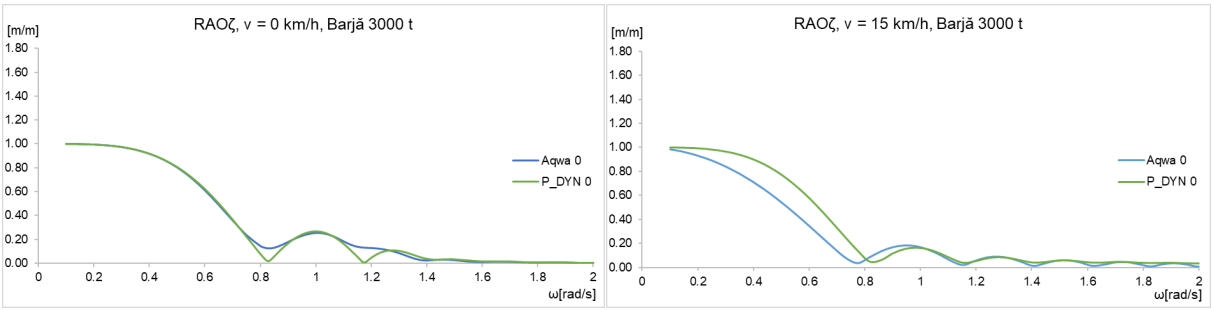

Figure 6.1. Response amplitude operators (RAOζ), μ=0° - vertical oscillation. v=0 km/h (left), v=15 km/h (right). 3000 TDW barge, full load.

6.1.2 Roll oscillation

For roll oscillations, the results show very good agreement between the two methods at low frequencies and zero speed. At a speed of 15 km/h, the differences become more pronounced, with the 3D model showing more amplified responses. This indicates that the 3D model is better at capturing dynamic and nonlinear effects associated with roll motion, particularly at higher speeds and in oblique wave conditions. The observed differences are attributed to the different approaches to modeling hydrodynamic damping.

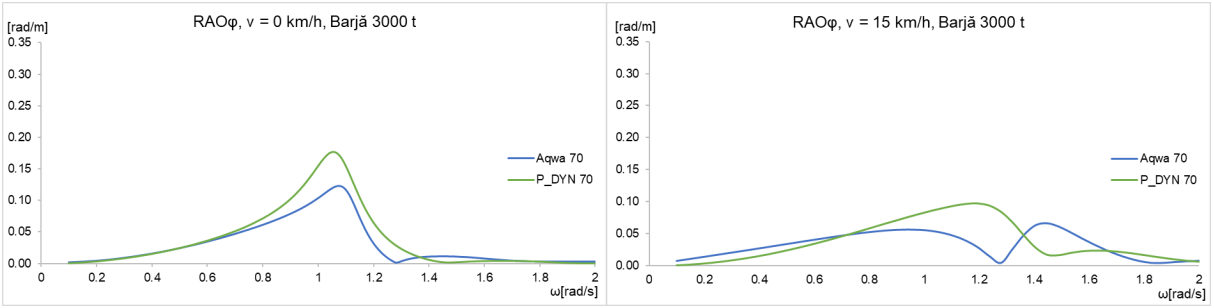

Figure 6.2. Response amplitude operators (RAOφ), μ=70° – roll oscillation. v=0 km/h (left), v=15 km/h (right). 3000 TDW barge, full load.

6.1.3 Pitch oscillation

Pitch oscillations show good correspondence between the two methods at low frequencies, but at higher frequencies and higher speeds, the 3D model again exhibits larger amplitudes. This indicates greater sensitivity to the hydrodynamic and inertial effects associated with pitch, especially at higher forward speeds. The differences observed between the two models at higher speeds suggest a significant influence of speed on the vessel's dynamic response.

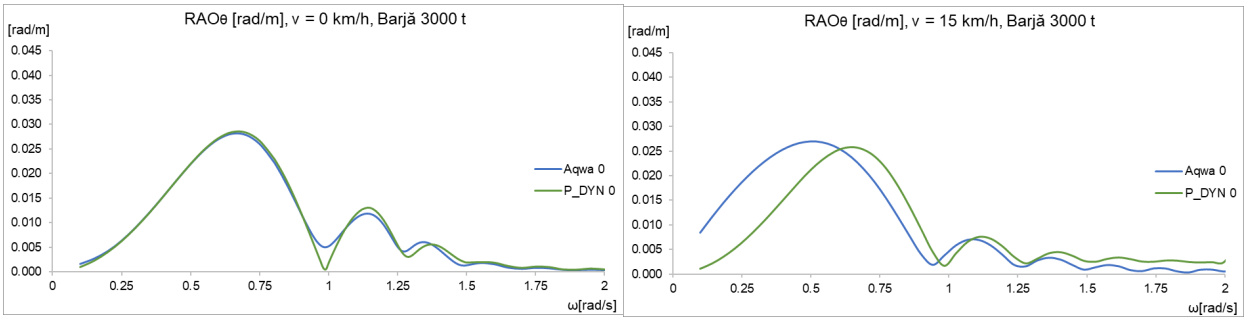

Figure 6.3. Response amplitude operators (RAOθ), μ=0° – pitch oscillation. v=0 km/h (left), v=15 km/h (right). 3000 TDW barge, full load.

6.1.4 Conclusions on the comparative analysis of motions using 2D-3D models

The comparative analysis revealed that both methods provide similar results at low frequencies and slow speeds, but the 3D model exhibited greater sensitivity at high frequencies and higher speeds, suggesting that it can better capture the complex interactions between waves and the hull. The differences between the two models become more pronounced at higher speeds, indicating that the 3D method offers a more detailed representation of dynamic phenomena, especially in resonance domains.

6.2 Short-term dynamic response analysis in random waves for the 3000 tdw barge

In this section, a short-term dynamic response analysis of the 3000 TDW barge in random waves was conducted for full load conditions. The vessel's motions, including vertical heave, pitch, and roll, were evaluated to determine if these movements fall within the safety limits set by seakeeping criteria. Additionally, the vessel's maximum accelerations were analyzed to assess the effects on cargo and the structural safety of the ship.

The results showed that, for most operating conditions, the vessel's motions and accelerations remain within acceptable limits. However, under large wave conditions and high speeds, vertical heave and pitch motions approached safety limits. In such conditions, careful management of forward speeds is required to prevent risks to the vessel's stability and structural integrity.

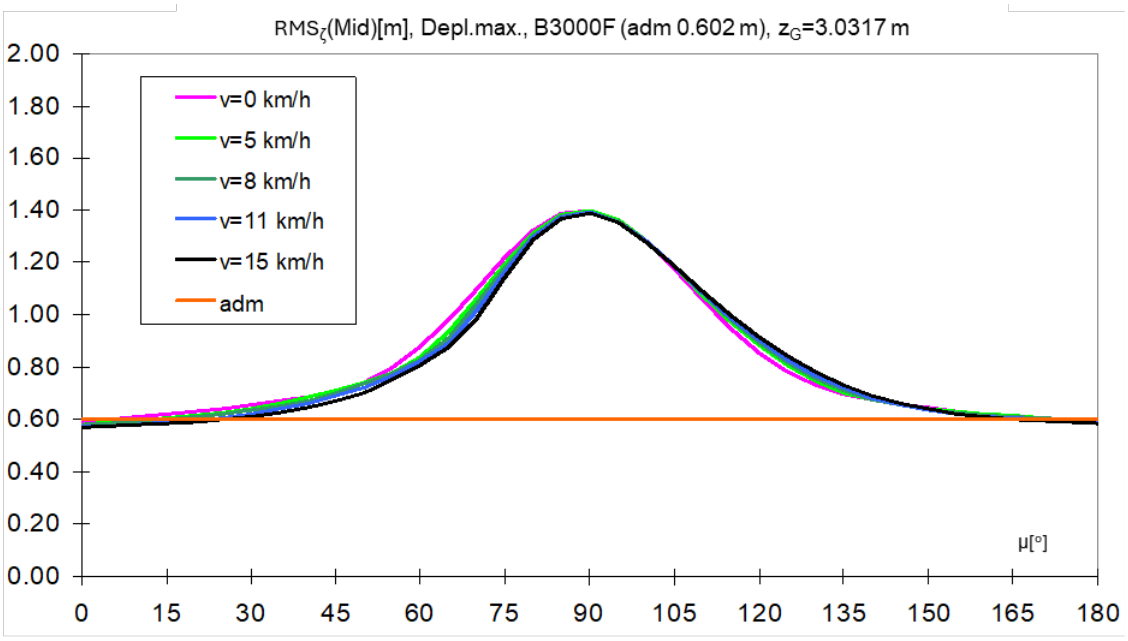

Figure 6.4. RMS maximum - Combined vertical heave and roll motion at midship, v=0-15 km/h, zG=3.0317 m.

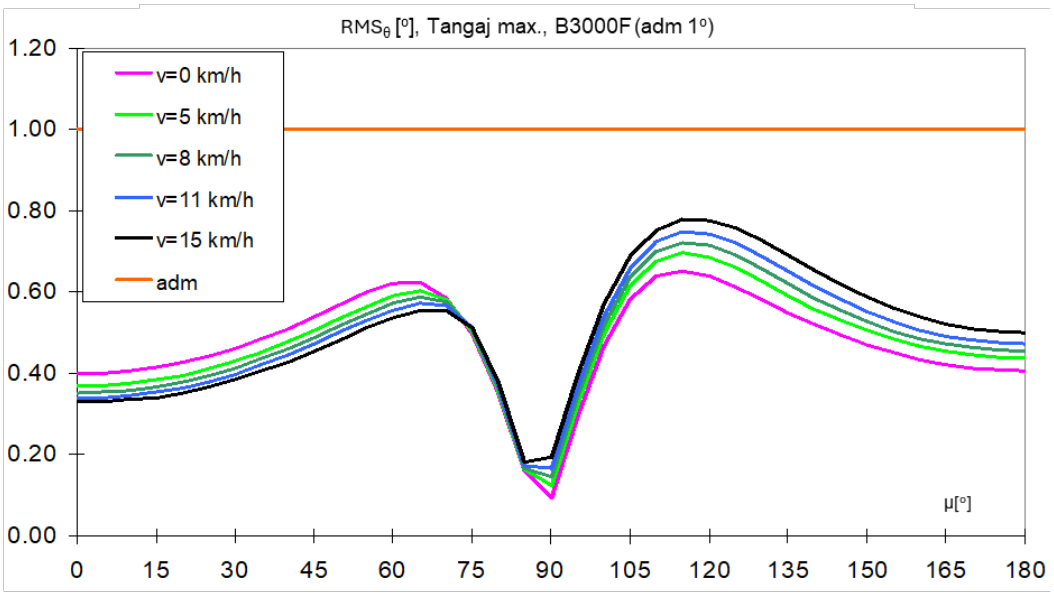

Figure 6.5. RMS maximum - Pitch motion, v=0-15 km/h.

In conclusion, the short-term dynamic response analysis showed that the 3000 TDW barge can operate safely in moderate wave conditions. However, in the case of severe waves or high speeds, careful monitoring of the vessel's motions and speed adjustments are necessary to ensure operational safety.

Chapter 7

ANALYSIS OF THE DYNAMIC BEHAVIOR OF A RIVER-COASTAL BOAT IN WAVES

7.1 Numerical model data for the oscillation analysis of the river-coastal vessel

This section presents the data of the numerical model used for the analysis of oscillations of the river-coastal vessel, including vertical heave, pitch, and roll motions. The model was created using the P_DYN software, and simulations were performed for speeds ranging from 0 to 15 knots, with varying ship-wave incidence angles between 0° and 180°. The motions were analyzed using response amplitude operators (RAO), and for roll motion, the effect of additional damping with and without bilge keels was included. The simulation results showed a good correlation between the numerical model and the vessel's dynamic behavior in regular wave conditions, providing useful data for evaluating the vessel's performance in various operational scenarios.

7.2 Amplitude response operator functions for the oscillations of the river-coastal vessel

For vertical heave motion, the RAO functions showed a moderate amplification of the vessel's response at ship-wave incidence angles of 0° and 45°, while at angles of 135° and 180°, the response amplified significantly, especially at higher speeds. In the case of pitch motion, there was an increase in amplitudes at higher speeds and oblique angles, particularly at 180°, where the amplitudes reached their maximum values. Roll motion was influenced by the position of the center of gravity and the presence of bilge keels, with amplitudes being more pronounced at higher speeds and without additional damping.

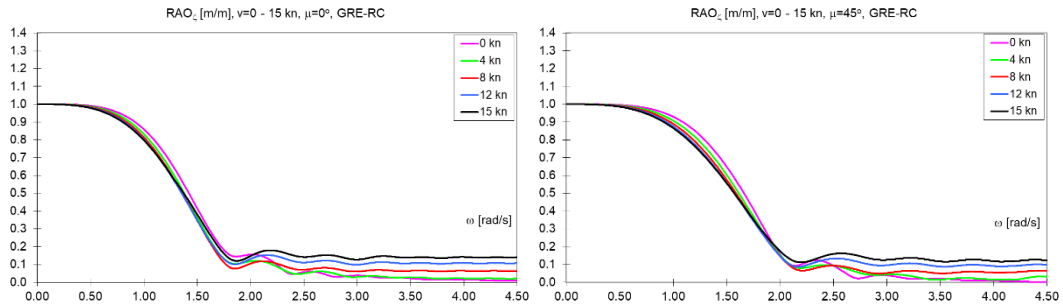

Figure 7.1. RAO - Vertical heave motion, v=0-15 knots, μ=0°, μ=45°.

7.3 Short-term dynamic response to oscillations of the river-coastal vessel

The short-term dynamic response of the vessel in random waves was analyzed using the ITTC wave spectrum. Vertical heave, pitch, and roll motions, along with the accelerations associated with these movements, were evaluated. RMS (Root Mean Square) values showed that vertical motions were amplified at ship-wave incidence angles close to 90°, while pitch and roll motions reached their maximum values at angles of 135° and 180°. Additionally, accelerations progressively increased at higher speeds, especially for pitch and roll motions, exceeding allowable limits under certain conditions.

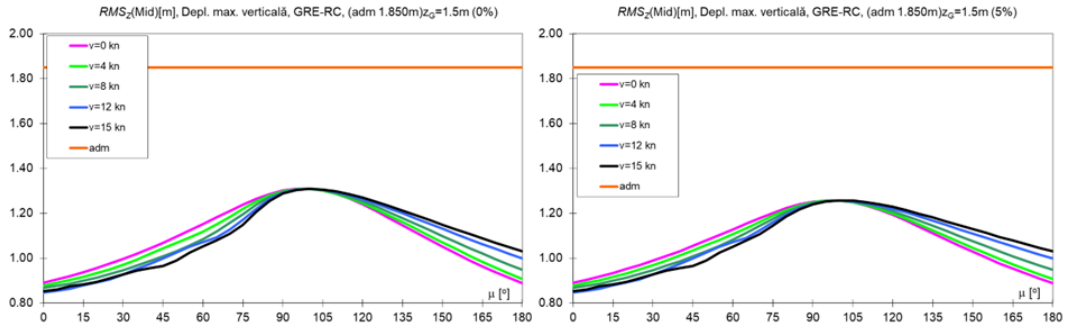

Figure 7.2. RMS maximum - Combined vertical heave and roll motion at midship, v=0-15 knots, zG=1.5 m, damping 0-5%.

7.4 Short-term operational limits of the river-coastal vessel

The operational limits of the vessel were established based on the significant wave height (Hs limit) and the Beaufort scale (B limit), depending on navigation speed and ship-wave incidence angle. As speed increases, operational limits decrease, especially at critical angles of 90° and 135°. At higher speeds, Hs limits drop below 0.8 meters, and the Beaufort scale drops below level 1 at critical angles, indicating reduced dynamic performance of the vessel in strong wave conditions and at high speeds. The additional damping provided by bilge keels slightly improved these limits, but their overall influence was limited.

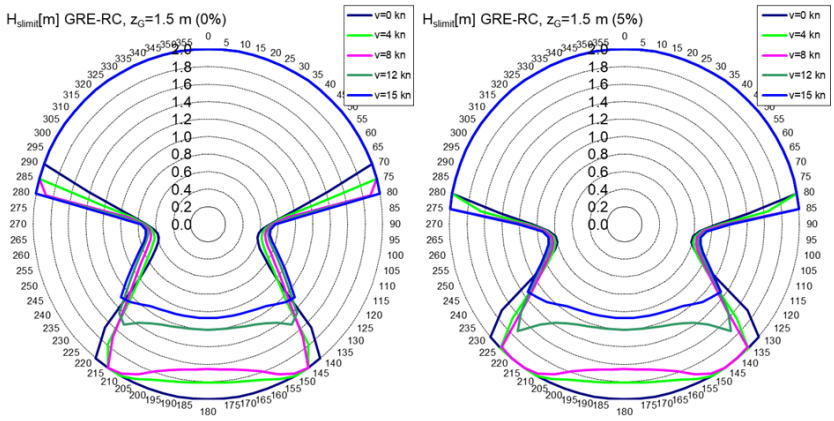

Figure 7.3. H_{slimit} - Operational limits, significant wave heights, v=0-15 knots, zG=1.5 m, additional roll damping 0-5%.

7.5 Conclusions on the dynamic analysis of the river-coastal vessel

The dynamic analysis highlighted that roll motions are the most sensitive to navigation speed and ship-wave incidence angle. As speed increases, the amplitudes of motions and accelerations rise significantly, especially at oblique angles. The position of the center of gravity significantly influences roll motions, with a lower position amplifying oscillations. The implementation of bilge keels reduced the oscillation amplitudes but failed to eliminate the negative effects under strong wave conditions and high speeds. In conclusion, navigation speed, ship-wave incidence angle, and the center of gravity position are essential factors in optimizing the vessel's dynamic performance.

Chapter 8

ANALYSIS OF THE STRUCTURAL RESISTANCE OF A 3000 TDW RIVER BARGE TO IMPACT FROM GROUNDING

8.1 Context of impact analysis from grounding in inland navigation

River navigation often takes place in shallow waters and on waterways that may present underwater obstacles, increasing the risk of grounding. Grounding impact is a critical issue for river barges, especially when they are fully loaded. Grounding can cause significant structural damage, affecting both the vessel's structure and the transported cargo, leading to substantial economic losses. This chapter presents a detailed analysis of the impact of grounding, considering its effects on a 3000 TDW barge, a common type of vessel used for river transport.

8.2 Structural evaluation of the 3000 tdw river barge subjected to grounding impact loads in the central cargo hold area

8.2.1 Navigation conditions on inland waters

River barges often operate on inland waterways with variable depths, which exposes them to the risk of grounding in areas with insufficient depth. Navigational conditions are crucial in determining the risk of grounding and the severity of the impact, including factors such as water depth, vessel speed, and the nature of the riverbed.

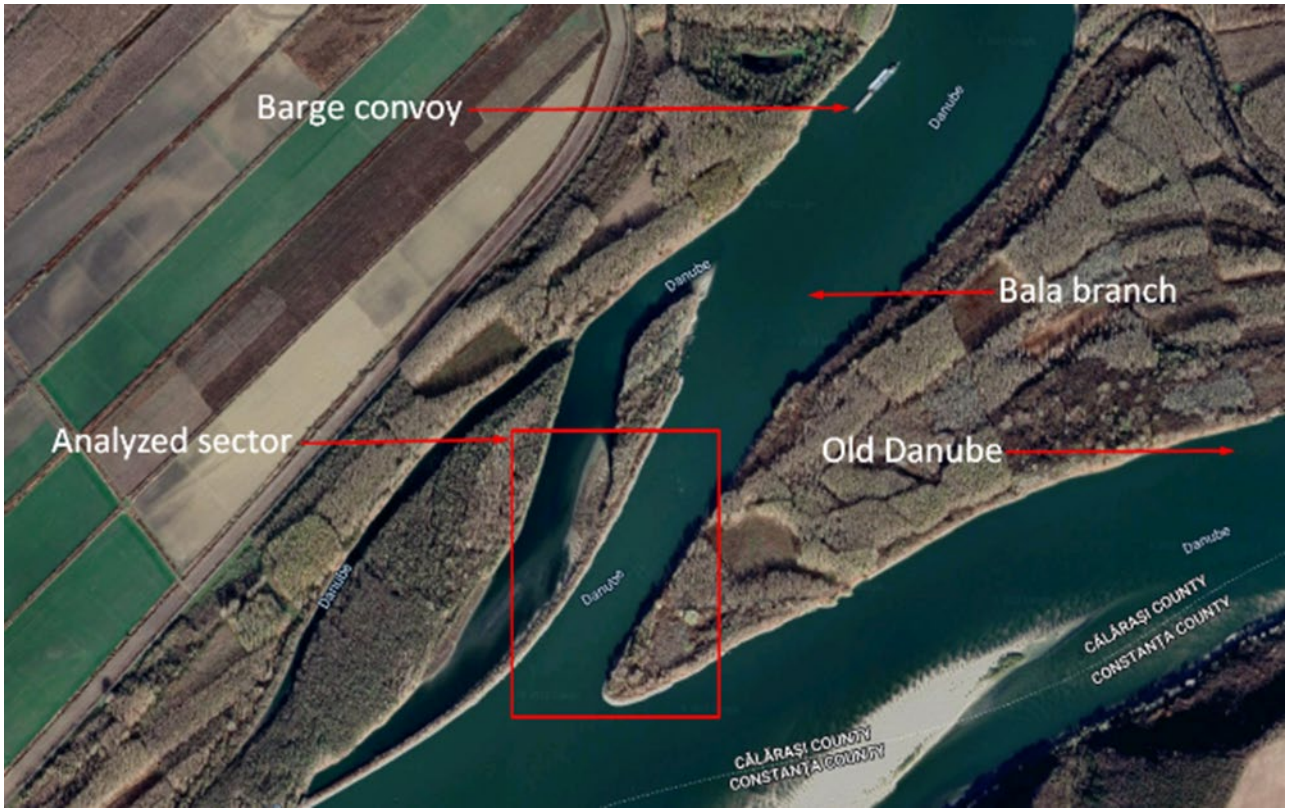

Figure 8.1. Location of the Bala branch (N 44.1906, E 27.5689, Google Maps) [126][127].

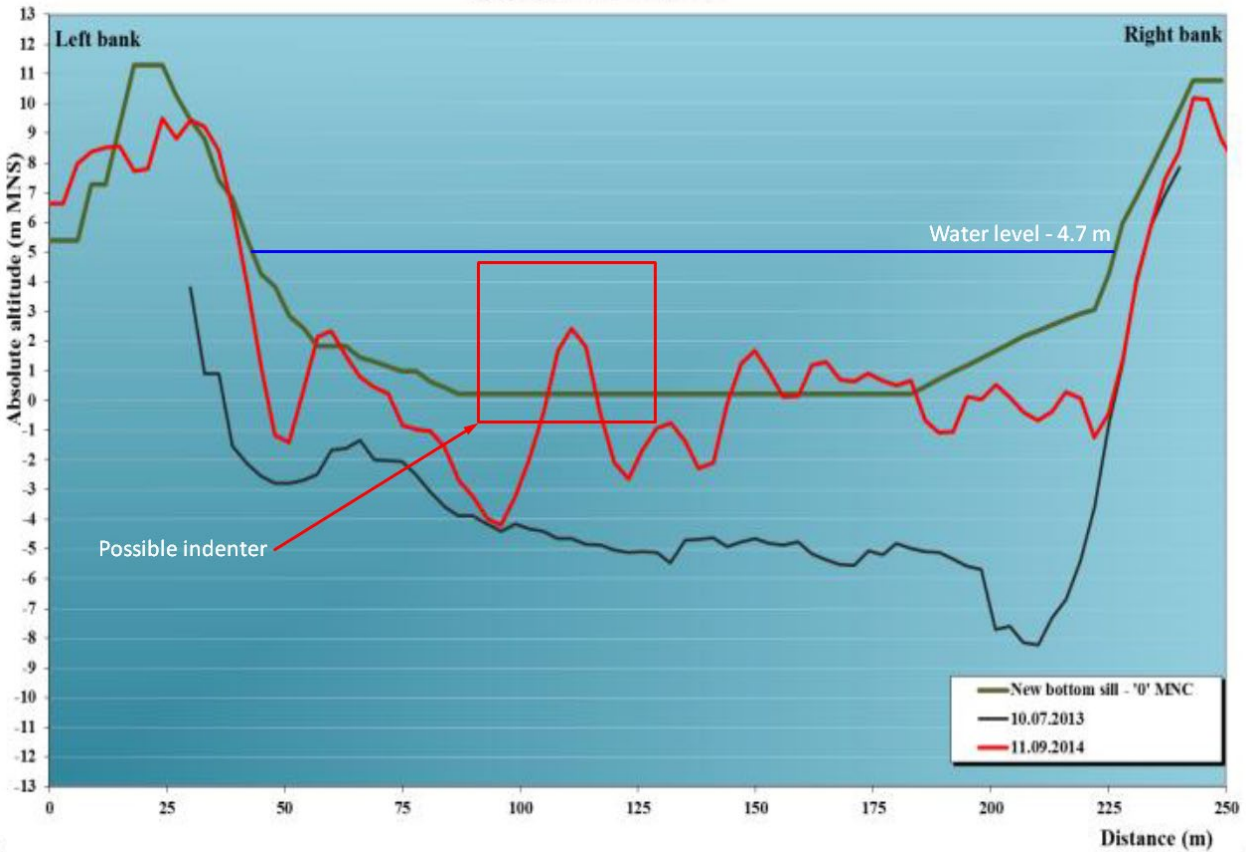

Figure 8.2. Cross-section of the Danube riverbed, 2013-2014. [126]

8.2.2 3D-FEM structural model and material of the 3000 tdw barge

To evaluate the structural behavior of the barge following impact, a 3D-FEM model of the midship section was created. The model included key structural details such as longitudinal and transverse beams, bulkheads, and stiffeners. The material used for the vessel's structure was steel, with its properties defined according to the standards of naval classification societies.

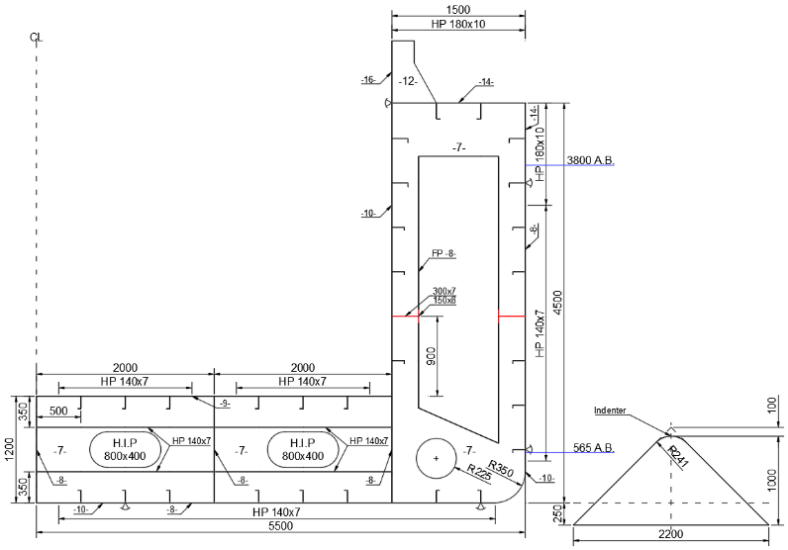

Figure 8.3. Midship cross-section, cargo hold, 3000 TDW barge.

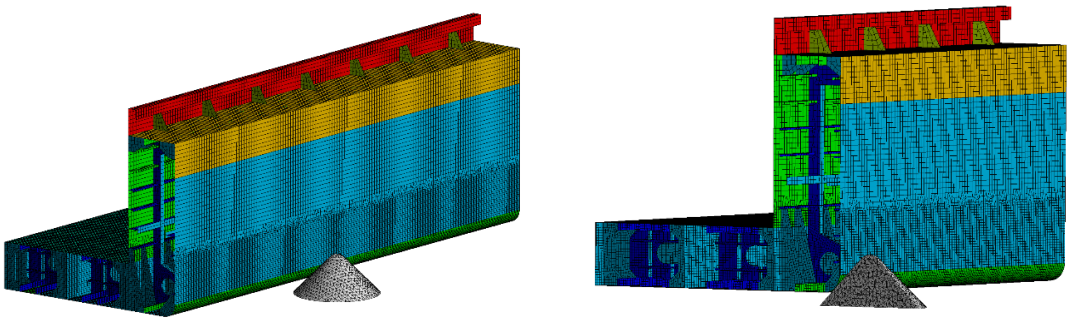

Figure 8.4. Geometry discretization. Complete 3D-FEM model (left), cross-section through the impactor (right).

8.2.3 Impact analysis from grounding in the central area of the barge

The simulations showed that maximum stresses occur in the double bottom and in the longitudinal bulkheads near the point of impact. Depending on the impact speed and the grounding angle, localized structural failure was observed. In full-load navigation scenarios, stresses reached higher values, indicating an increased risk of severe structural damage in the midship area.

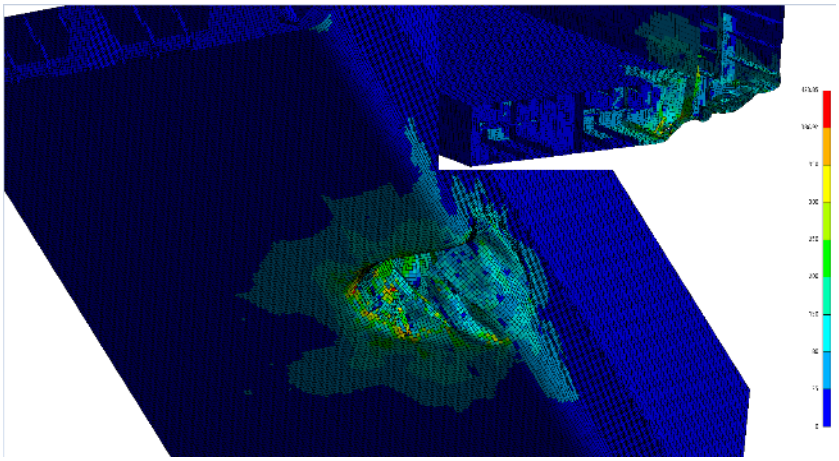

Figure 8.5. Von Mises stresses (MPa), Case A3 - Full Load - FEM Model without Preloading, 3000 TDW barge.

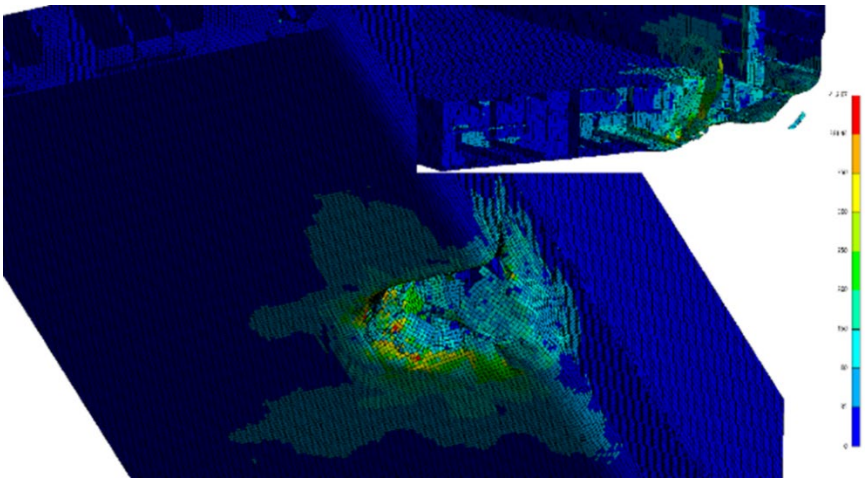

Figure 8.6. Von Mises stresses (MPa), Case A4 - Full Load - FEM Model with Preloading, 3000 TDW barge.

8.2.4 Conclusions

The results indicate that the midship area of the barge is vulnerable to damage in the event of grounding, and the structural behavior depends on the impact speed and the cargo being transported. Protective measures, such as reinforcing the double bottom, could reduce the risk of major damage under these conditions.

8.3 Structural evaluation of the 3000 tdw river barge subjected to grounding impact loads in the bow area

8.3.1 3D-FEM structural model and grounding conditions

The structural model of the bow was developed to analyze the impact of grounding in this area, considered critical due to hydrodynamic motions. Grounding scenarios with various speeds and impact angles were simulated to evaluate the structural strength under grounding conditions.

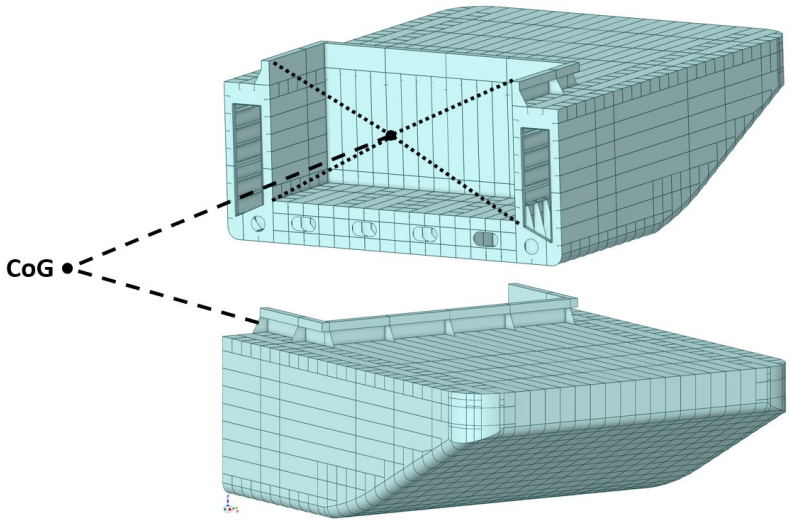

Figure 8.7. 3D CAD model of the bow, 3000 TDW barge.

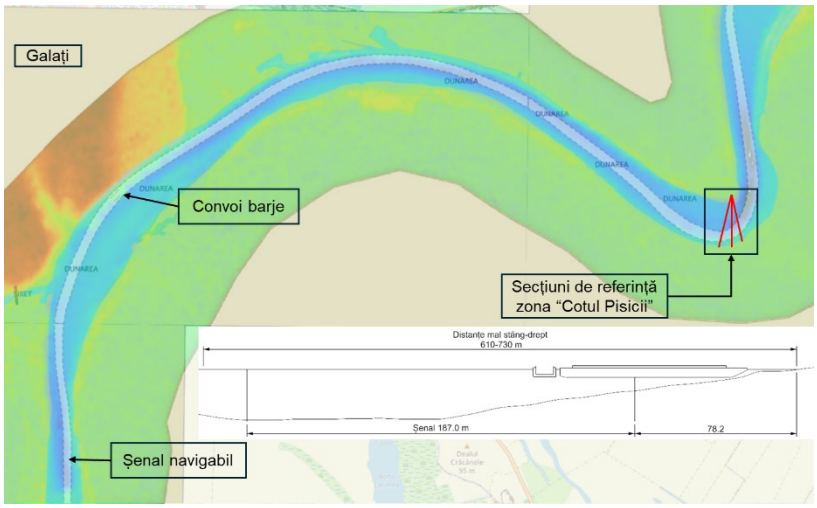

Figure 8.8. Navigation chart overlaid on 3D scan. Galați area. Position of the barge in the riverbed cross-section.

8.3.2 Impact analysis from grounding in the bow area of the barge

The results indicate a more uniform distribution of stresses in the bow area compared to the midship section. The specific geometry of the bow favors sliding during grounding, which limits the severity of damage. However, at high speeds and in rough navigation conditions, the stresses can exceed allowable limits, highlighting the need for additional structural protection measures.

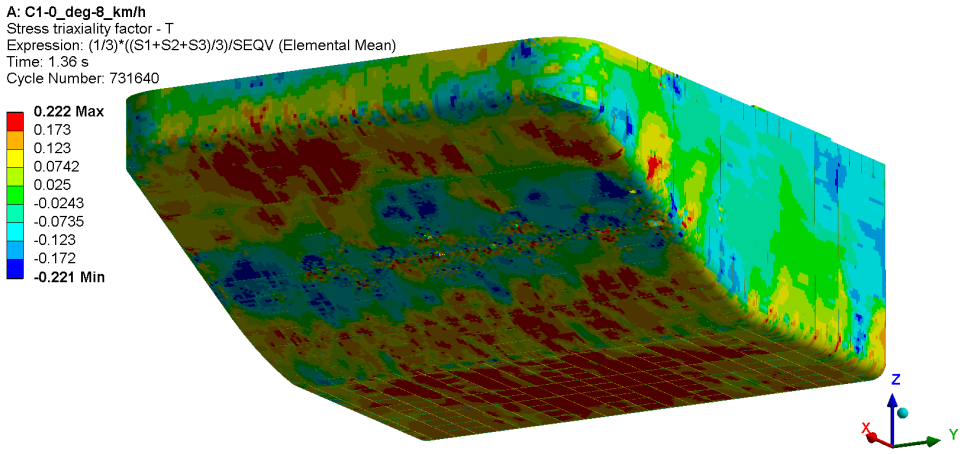

Figure 8.9. Distribution of the triaxiality factor. Case 1. M=0°, v=8 km/h. Grounding impact at the bow of the 3000 TDW barge.

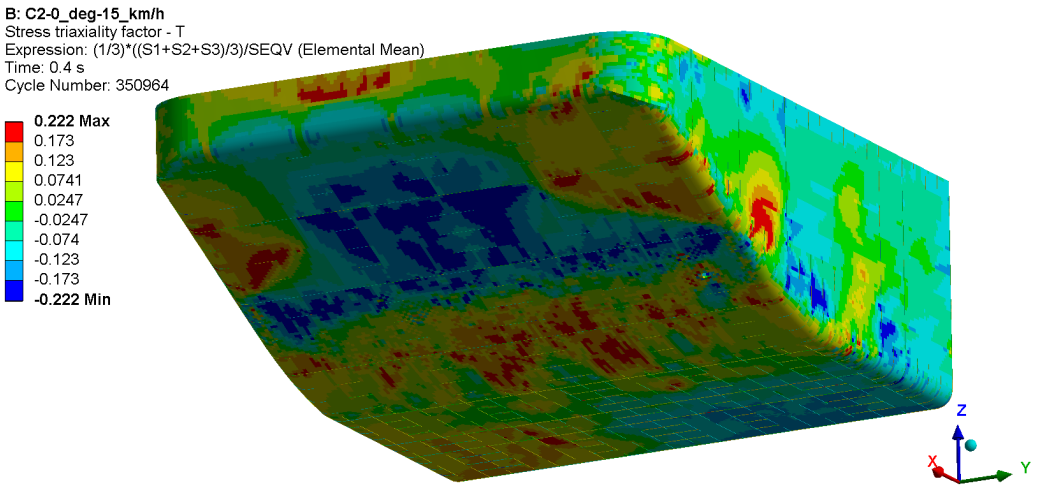

Figure 8.10. Distribution of the triaxiality factor. Case 2. μ=0°, v=15 km/h. Grounding impact at the bow of the 3000 TDW barge.

8.3.3 Conclusions

The bow area of the 3000 TDW barge exhibits better resistance to grounding compared to the central section. Although the bow's geometry mitigates the impact severity, the risk of damage increases under high-speed operation or in environments with underwater obstacles, in strict relation with their geometrical shape and morphology.

8.4 Structural evaluation of the 3000 tdw barge subjected to grounding impact loads in the central area, considering the effect of vertical oscillations in waves

8.4.1 Structural models and cases analyzed

For this analysis, vertical oscillations induced by waves on the 3000 TDW barge were considered. FEM models were modified to include wave-induced oscillations, and several impact scenarios with waves were simulated, both under ballast conditions and full load.

Tabel 8.3. Description of the analyzed cases.

Case	Bottom area framing system	Side framing system	μ [°]	v_x [m/s]	v_y	v_z
C1	Longitudinal	Transversal	180°	-	-	0.455
C2		Longitudinal		-	-	
C3		Transversal		4.167	-	
C4		Longitudinal			-	
C5		Transversal	45°	2.946	2.946	
C6		Longitudinal				
C7		Transversal	30°	3.608	2.083	
C8		Longitudinal				

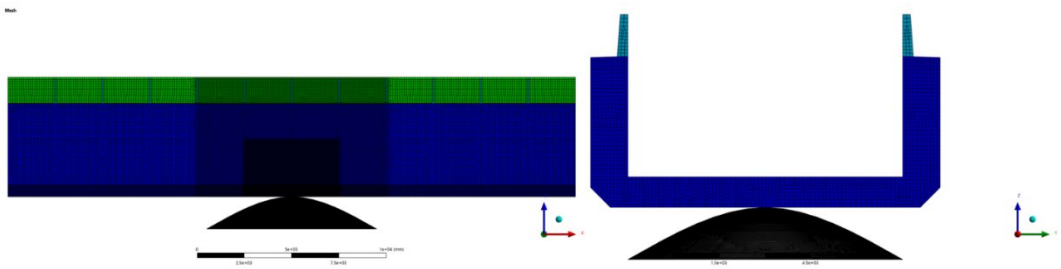

Figure 8.11. FEM model, master section area, 3000 TDW barge, SLO bottom, STO bulkheads (C1, C3, C5, C7).

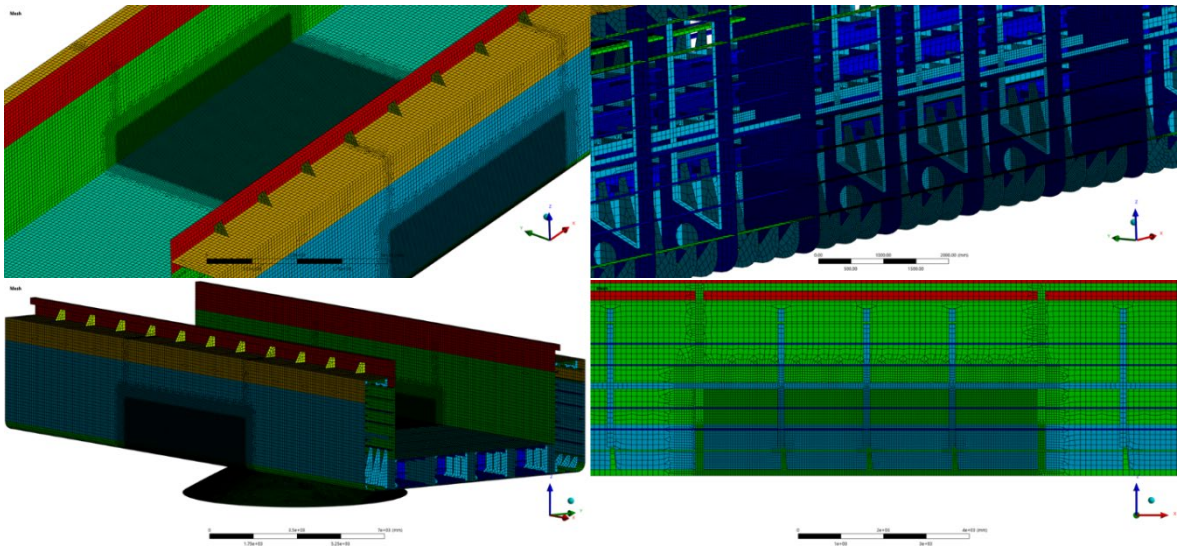

Figure 8.12. FEM model, master section area, 3000 TDW barge, SLO bottom, SLO bulkheads (C2, C4, C6, C8), discretization details.

8.4.2 Impact analysis results

The analysis highlighted the impact of vertical oscillations in the case of grounding impacts. In particular, large waves combined with the vessel's speed led to a proper assessment of stresses in critical areas of the barge. The oscillations contributed to an uneven distribution of loads, identifying the risk of structural failure in certain parts of the vessel.

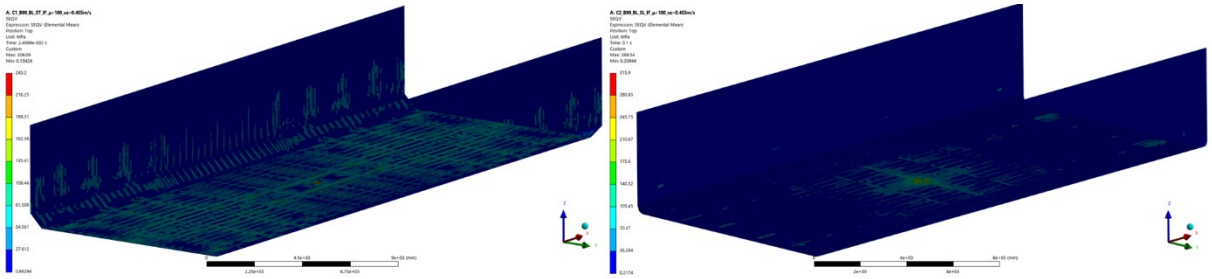

Figure 8.13. C1-C2, 3000 TDW barge, σvM - von Mises stress, outer shell.

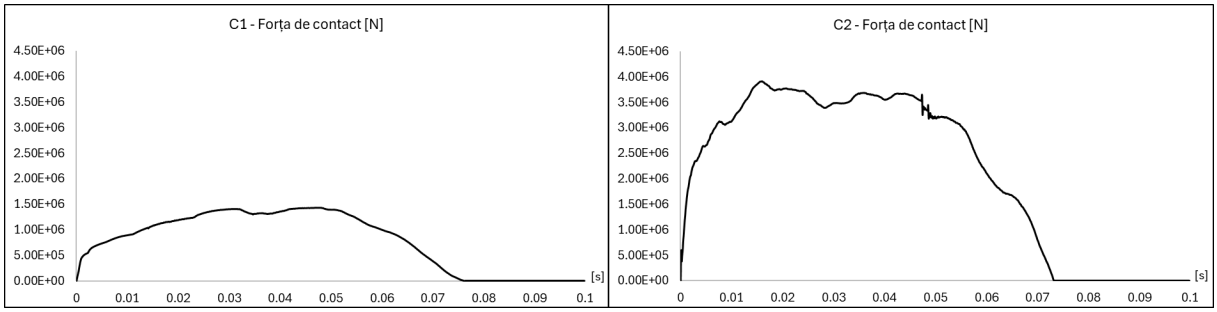

Figure 8.14. C1-C2, 3000 TDW barge, contact force at impact.

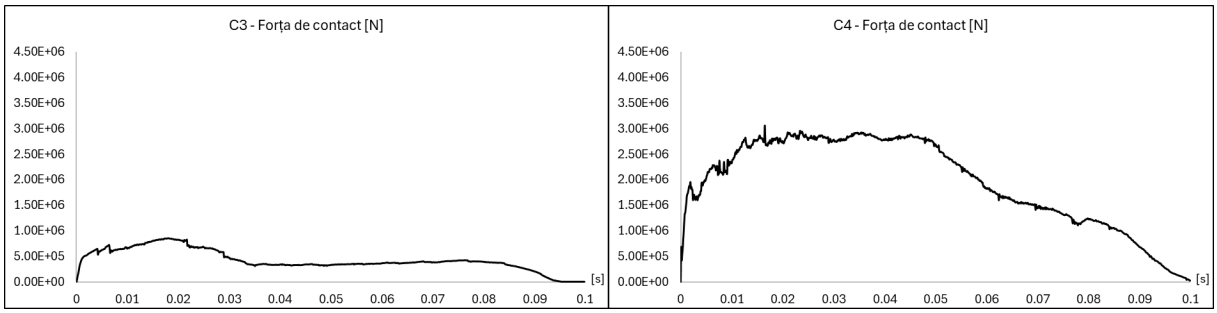

Figure 8.15. C3-C4, 3000 TDW barge, contact force at impact.

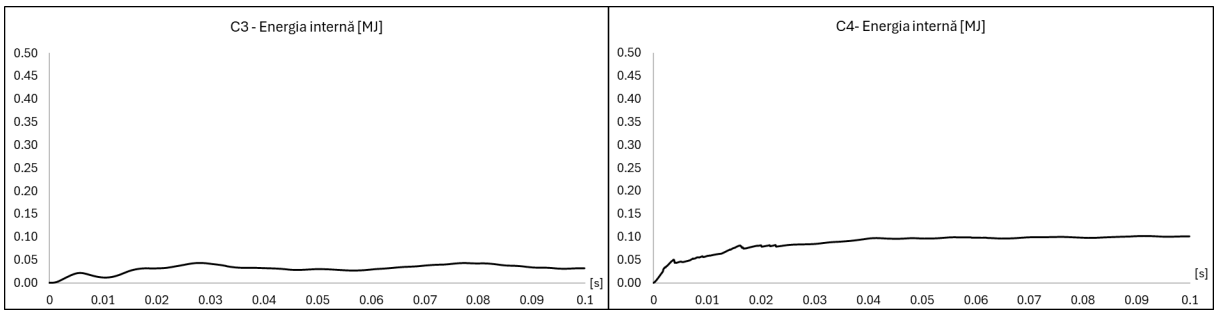

Figure 8.16. C3-C4, 3000 TDW barge, internal deformation energy.

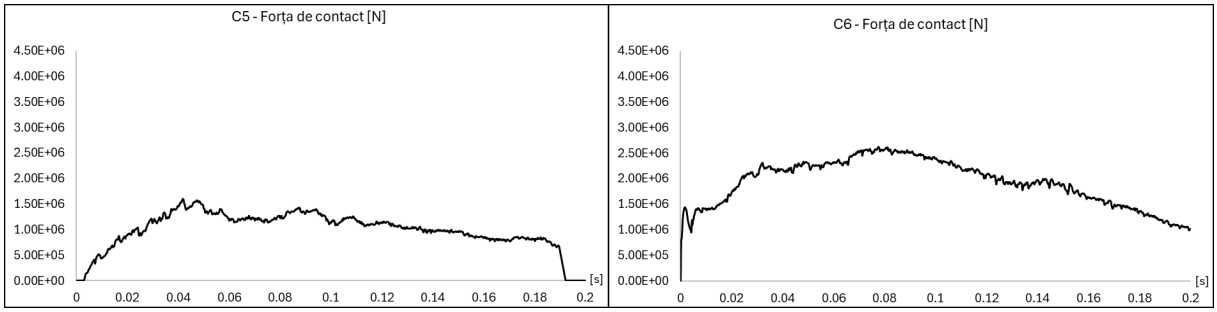

Figure 8.17. C5-C6, 3000 TDW barge, contact force at impact.

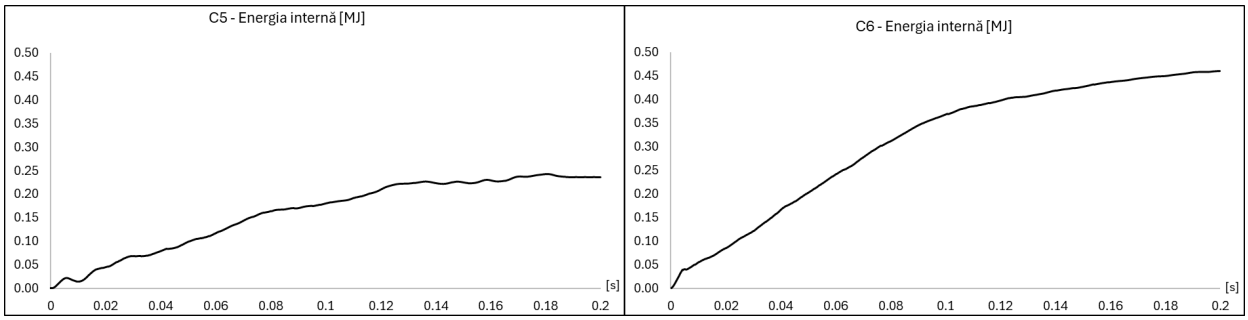

Figure 8.18. C5-C6, 3000 TDW barge, internal deformation energy.

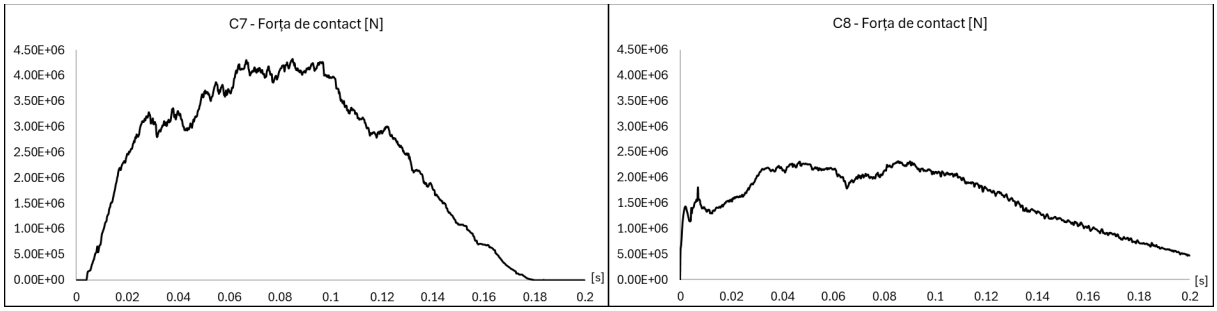

Figure 8.19. C7-C8, 3000 TDW barge, impact contact force.

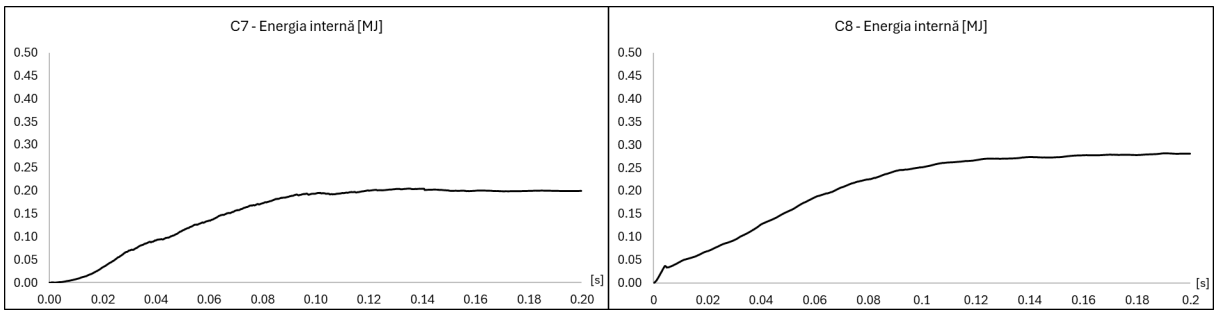

Figure 8.20. C7-C8, 3000 TDW barge, internal deformation energy.

Tabel 8.5. Results of the grounding impact analysis considering the ship's movements, 3000 TDW barge. (failure criterion - specific strain limit of 0.1817 mm/mm)

Case		**C1**	**C2**	**C3**	**C4**	**C5**	**C6**	**C7**	**C8**
Direction of impact		**180°**	**180°**	**180°**	**180°**	**45°**	**45°**	**30°**	**30°**
σ_{vM}	[Mpa]	308.71	372.59	>410	>410	>410	>410	>410	>410
σ_x	[Mpa]	226.55	322.86	-344.9	-385.5	-407.9	>410	307.28	365.92
σ_y	[Mpa]	250.17	353.29	327.98	361.75	>-410	>410	-395.16	-373.76
σ_z	[Mpa]	-216.98	408.76	>-410	376.06	>-410	>410	>-410	386.2
τ_{xy}	[Mpa]	91.93	173.06	134.03	-289.65	-133.26	213.31	-194.87	133.95
τ_{yz}	[Mpa]	-118.66	207.83	174.39	164.06	299.86	240.84	-201.12	177.92
τ_{xz}	[Mpa]	-70.25	149.73	212.53	242.85	-211.6	210.71	-210.91	-191.69
ε_p	[mm/mm]	0.066	0.1255	**0.1817**	**0.1817**	**0.1817**	**0.1817**	**0.1814**	**0.1817**
E_c	[MJ]	0.374	0.374	31.7	31.7	31.7	31.7	31.7	31.7
E_i	[MJ]	0.045	0.044	0.044	0.102	0.24	0.461	0.205	0.2817
Shell penetration	-	0	0	0	1	1	1	1	1
Failed elements	-	0	0	1	101	70	109	362	77
δ_Z	[mm]	11	13	11	63	219	285	166	191

8.5 Structural evaluation of the GRE-RC vessel subjected to grounding impact loads in the bow area, considering the effect of vertical oscillations in waves

8.5.1 Structural model and cases analyzed

The GRE-RC vessel, made of composite materials, was subjected to a similar impact analysis as the barge, with simulations including vertical oscillations induced by waves. The composite material was modeled to reflect its specific behavior under impact loading conditions.

Tabel 8.6. Analyzed cases, GRE-RC vessel.

Case	**μ [°]**	**vx**	**vy [m/s]**	**vz**
C1-A	180°	7.716	-	-
C2-A			-	1.000

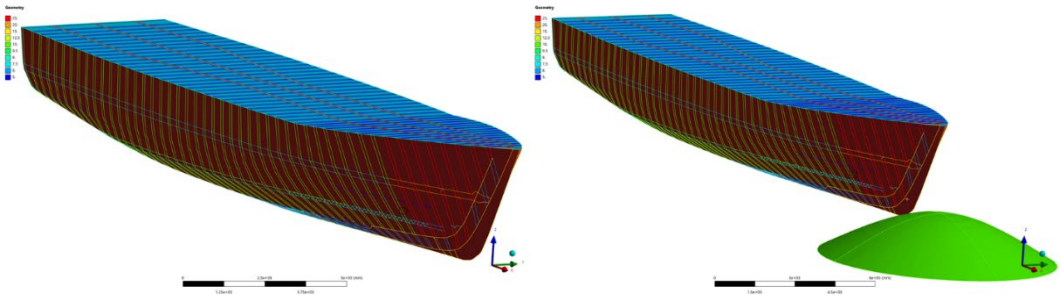

Figure 8.21. CAD geometry, GRE-RC vessel.

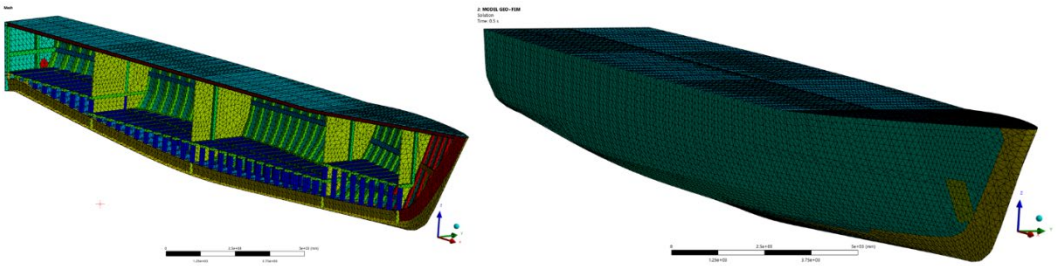

Figure 8.22. FEM model, GRE-RC vessel.

8.5.2 Impact analysis results

Composite materials behaved differently from metallic ones in the case of grounding impact. The results indicated better energy absorption due to the material's elasticity, leading to a more uniform distribution of stresses. Vertical oscillations had a moderate effect on damage in the GRE-RC vessel due to the specific rigidity of the composite material.

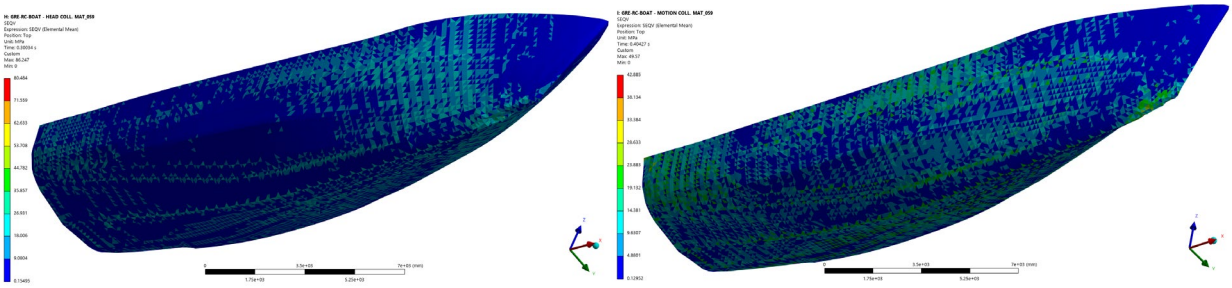

Figure 8.23. C1-A - C2-A, GRE-RC vessel, σvM - von Mises stress, outer shell.

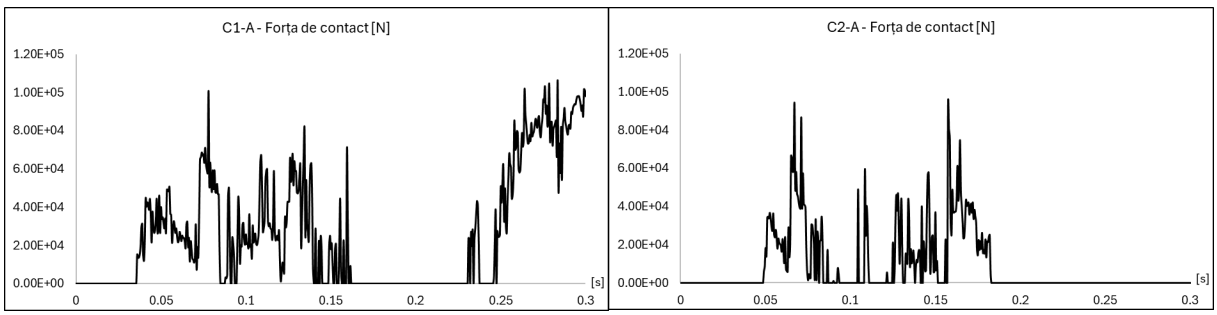

Figure 8.24. C1-A - C2-A, GRE-RC vessel, impact contact force.

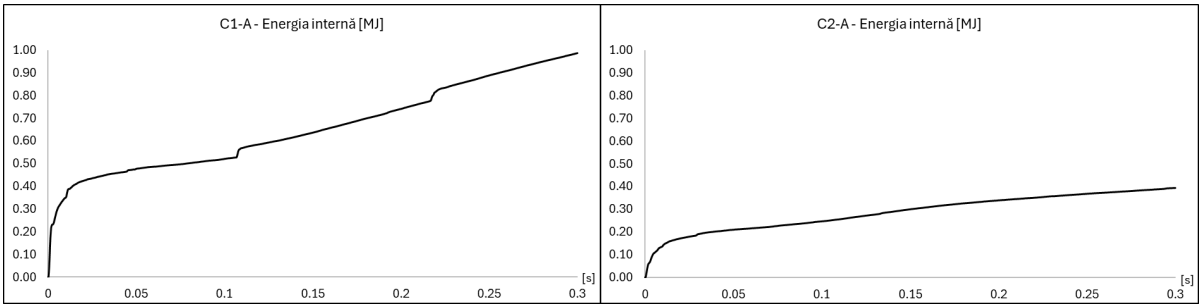

Figure 8.25. C1-A - C2-A, GRE-RC vessel, internal deformation energy.

Chapter 9

FINAL CONCLUSIONS AND PERSONAL CONTRIBUTIONS

9.1 Final conclusions

The Galati area, located on the Danube, is a key point for maritime traffic in Romania, having a major influence on the regional and national economy. The study of maritime safety and accidents in this area revealed that groundings are the most frequently reported incidents. They typically involve river barges, highlighting specific vulnerabilities in inland waterway navigation. These groundings lead to structural damage, underscoring the need for advanced structural modeling methods for risk assessment and management.

1. The analysis of current research (Chapter 1) shows that the assessment of structural risks associated with accidental loads on ships has significantly improved due to numerical modeling and experiments. Simulations conducted by researchers such as Pedersen, Simonsen, and Ehlers have highlighted that groundings introduce extreme loads into the ship's structure, especially in large vessels such as oil tankers. The use of the finite element method (FEM) has allowed for accurate assessment of the ship's structural behavior in failure scenarios but requires significant preparation efforts.

2. The analysis of theoretical foundations for understanding the strength of naval structures (Chapter 2) focused on using CAD/FEM modeling to analyze both global and local ship strength. Case studies included an LNG carrier and a river tug. The strength assessment stages involve calculating wave pressures applied to the ship's structure and identifying critical stress points. Additionally, the behavior of ships under oscillations and structural impacts was analyzed.

3. The validation of numerical models used for oscillation simulations and structural impact analysis (Chapter 3) confirmed their effectiveness in evaluating the dynamic behavior of ships. Comparisons between numerical methods and experimental results showed good correlation but also indicated some limitations in capturing nonlinear radiation and diffraction effects.

4. The structural strength analysis of a 3000 TDW river barge (Chapter 4) was conducted using both 1D modeling and detailed 3D-FEM simulations. The study evaluated the barge's behavior under different loading scenarios and oblique waves, identifying stress concentrators in structural transition areas, suggesting the need for improvements to prevent damage.

5. The structural performance of a river vessel made of composite materials was analyzed comparatively (Chapter 5). Two composite materials (A1 and A2) were evaluated under various loading conditions. Material A2 exhibited superior performance in all scenarios. The 3D-FEM analysis showed that the vessel made of material A2 met stress and deformation limits in all operating conditions.

6. The dynamic behavior of a 3000 TDW barge in waves (Chapter 6) was analyzed using advanced numerical methods, comparing P_DYN and Ansys Aqwa methods. The results showed that Ansys Aqwa models hydrodynamic interactions at high speeds more comprehensively. It was also found that the barge is sensitive to transverse waves, imposing restrictions on safe operation in high waves.

7. The analysis of the dynamic behavior of a composite material river vessel in random waves (Chapter 7) highlighted the importance of adjusting the advance speed and center of

gravity position to optimize dynamic performance. Roll fins significantly reduced roll oscillations, and the analysis showed that the vessel's oscillations are most sensitive to these movements.

8. The impact analysis for two types of vessels (Chapter 8) assessed the structural strength of a river barge and a composite material river-coastal vessel. The study included vertical movements of the vessels in impact scenarios, allowing for a more realistic assessment of structural damage. The results showed that barges with transverse framing distributed impact loads better, while longitudinal framing structures were more prone to penetration and damage.

The overall conclusion of the study is that including ship movements in grounding impact simulations provides a more realistic and accurate assessment of structural damage risks. This innovative approach contributes to improving ship design, making them more resilient in extreme operating conditions.

9.2 Personal Contributions

1. The extensive study of the current state of research in the field: The work provided a detailed analysis of the literature on structural risks and maritime accidents, highlighting advancements in the use of numerical simulations for analyzing the structural behavior of ships. Historically, empirical methods dominated the analysis, but recent developments have introduced more precise modeling techniques, such as FEM and three-dimensional hydrodynamic simulations.

2. Validation of numerical methods through experimental data: A major contribution was the validation of numerical models through comparisons with experimental data. This step allowed for adjustments to simulations and ensured a strong correlation between real behavior and numerical predictions. Emphasis was placed on comparing deformations and stresses obtained in simulations with experimental results, which strengthened the credibility of the methods used.

3. Detailed global analyses: Complex global simulations were conducted for a 3000 TDW river barge and a 24 m composite vessel. The focus was on analyzing structural behavior under navigation and grounding conditions, including various loading and impact scenarios. These simulations provided a clear perspective on the resistance and structural behavior of vessels in operational conditions.

4. Analysis of ship dynamics and estimation of short-term maximum response: The study thoroughly addressed ship movements in waves, analyzing vertical translation, pitch, and roll, providing predictions on dynamic behavior in severe wave conditions. The integration of statistical methods allowed for a detailed assessment of ship movements, providing a solid foundation for evaluating operational safety.

5. Incorporation of short-term dynamic analyses into grounding impact assessments considering ship movements: An innovative contribution was the integration of ship's dynamic movements into grounding impact analyses. This allowed for a more realistic assessment of how the ship’s structure responds to impacts under realistic navigation conditions. The methodology offers solutions for optimizing ship design to prevent structural damage.

6. Comprehensive study for grounding impact analysis for inland barges and medium-sized vessels (24 m): The study included detailed simulations for two types of vessels, a river barge and a composite vessel, exploring how each structure responds to lateral and frontal impacts. This detailed analysis allowed for the identification of reinforcement solutions for structures vulnerable to impacts.

7. Conclusions regarding the effect of considering ship movements in grounding impact analysis: Integrating ship movements into impact analyses showed that they can significantly influence the distribution of stresses and deformations in the ship's structure, suggesting the need for implementing these assessments for safer design.

9.3 Future Directions

1. Development of advanced numerical methods: It is necessary to improve numerical methods through more precise simulation of nonlinear phenomena and structure-fluid interactions. Technologies such as artificial intelligence and machine learning can accelerate simulations and optimize risk assessment processes.

2. Expansion of experimental validation through full-scale testing: Future research should include full-scale testing to ensure more rigorous validation of numerical methods, exploring nonlinear effects and complex interactions between structures and the marine/fluvial environment.

3. Integration of climatic and environmental effects: Climate change and extreme weather phenomena must be integrated into simulations to accurately assess their impact on ship safety.

4. Optimization of ship design based on integrated analyses: The study's conclusions suggest that ship design can be optimized by incorporating dynamic simulation results into the design stages to prevent structural damage and improve ship performance.

5. Research on new materials for ship construction: The development of advanced materials, such as aluminum alloys or hybrid composites, can offer innovative solutions for enhancing ship strength and safety.

6. Improvement of real-time structural monitoring: Real-time monitoring technologies should be expanded to detect damage in the early stages and prevent operational risks, by integrating sensor systems and artificial intelligence algorithms.

7. Detailed investigation of ship behavior in extreme waves: Future research should focus on simulating ships in extreme wave scenarios, exploring how ship structures and performance are affected by extreme navigation conditions.

Selective References

[1] EMSA, *Annual Overview of Marine Casualties and Incidents 2019*, 2019.
[2] EMSA, *Marine Casualties and Incidents » Incident Data*, 2020. [Online]. Valabil la: https://gisis.imo.org/Public/MCI/Browse.aspx?Form=Incident&Action=View&IncidentID=10319
[3] Www.fleetmon.com, *Major oil spill off Mauritius Island | WAKASHIO - FleetMon Maritime News*, 2020. https://www.fleetmon.com/maritime-news/2020/30533/major-oil-spill-mauritius-island/ (data accesării 12 septembrie 2020).
[4] SAFETY4SEA, *Sanchi: The world’s worst oil tanker disaster in decades - SAFETY4SEA*, 2018. https://safety4sea.com/cm-sanchi-the-worlds-worst-oil-tanker-disaster-in-decades/ (data accesării 12 septembrie 2020).
[5] Anchorage Daily News, *30 years after the Exxon Valdez, have Alaskans forgotten its most important lessons? - Anchorage Daily News*, 1989. https://www.adn.com/opinions/2019/03/23/30-years-after-the-exxon-valdez-have-alaskans-forgotten-its-most-important-lessons/ (data accesării 12 septembrie 2020).
[6] P. T. Pedersen, *Ship grounding and hull-girder strength*, *Mar. Struct.*, vol. 7, nr. 1, pp. 1-29, ian. 1994, doi: 10.1016/0951-8339(94)90008-6.
[7] B. C. Simonsen, *Mechanics of Ship Grounding Department of Naval Architecture And Offshore Engineering*, 1997.
[8] O. Kitamura, *FEM approach to the simulation of collision and grounding damage*, *Mar. Struct.*, vol. 15, nr. 4-5, pp. 403-428, 2002, doi: 10.1016/S0951-8339(02)00010-2.
[9] H. S. Alsos și J. Amdahl, *On the resistance of tanker bottom structures during stranding*, *Mar. Struct.*, vol. 20, nr. 4, pp. 218-237, oct. 2007, doi: 10.1016/j.marstruc.2007.06.001.
[10] T. H. Nguyen, J. Amdahl, L. Garrè, și B. J. Leira, *A study on dynamic grounding of ships*, în *Advances in Marine Structures - Proceedings of the 3rd International Conference on Marine Structures, MARSTRUCT 2011*, 2011, pp. 373-380. doi: 10.1201/b10771-46.
[11] DNV GL, *Rules for Classification of Ships, Part 6 Additional Class Notations, Chapter 2 Section 1*, nr. December, pp. 1-6, 2015.
[12] Bureau Veritas, *Rules for the classification of inland navigation vessels: Part B - Hull design and construction*, vol. 32, nr. November 2014, 2011, Data accesării: 13 martie 2021. [Online]. Valabil la: https://marine-offshore.bureauveritas.com/bv-rules
[13] ANR, *Autoritatea navală română*, 2020. https://portal.rna.ro/ (data accesării 1 septembrie 2020).
[14] D.-S. Perijoc, L. Domnișoru, și C. Angheluță, *On the methods for 3D-CAD-FEM modelling of a pusher structure*, nr. June, p. 2020, 2020.
[15] L. Domnișoru, *Special chapters on ship’s structures analysis. Applications*. Galati: The University Foundation „Dunarea de Jos” Galati Publishing House, 2017.
[16] L. Domnisoru, *On the Structural Valuation in Oblique Waves of a Large Liquefied Natural Gas Carrier By 3D-Fem Model Approach*, *Int. J. Mod. Manuf. Technol.*, vol. 15, nr. 2, pp. 200-219, 2023, doi: 10.54684/ijmmt.2023.15.2.200.
[17] L. Domnisoru și D.-S. Perijoc, *On the seakeeping response valuation in random sea state conditions of a large LNG liquefied natural gas carrier*, *Int. J. Mod. Manuf. Technol.*, 2024.
[18] Ansys Inc., *Ansys Aqwa User Manual*, 2012.
[19] *European agreement concerning the international carriage of dangerous goods by inland*

waterways (ADN), vol. I, nr. January. 2019. doi: 10.18356/91419305-en.

[20] E. Burlacu, L. Domnisoru, și D. Obreja, *SEAKEEPING PREDICTION OF A SURVEY VESSEL OPERATING IN THE CASPIAN SEA*, 2018.

[21] D. Obreja, *Survey Vessel Caspica. Model Resistance Tests, Report No. 617*, Galati, 2013.

[22] J. W. Ringsberg *et al.*, *MARSTRUCT benchmark study on nonlinear FE simulation of an experiment of an indenter impact with a ship side-shell structure*, *Mar. Struct.*, vol. 59, nr. February, pp. 142-157, 2018, doi: 10.1016/j.marstruc.2018.01.010.

[23] B. C. Cerik, J. W. Ringsberg, și J. Choung, *Revisiting MARSTRUCT benchmark study on side-shell collision with a combined localized necking and stress-state dependent ductile fracture model*, *Ocean Eng.*, vol. 187, p. 106173, sep. 2019, doi: 10.1016/j.oceaneng.2019.106173.

[24] D. S. Perijoc, L. Domnisoru, și C. M. Angheluță, *Grounding crashworthiness of an inland floating structure*, *Sci. Bull. Nav. Acad.*, vol. XXV, nr. 1, pp. 50-57, aug. 2022, doi: 10.21279/1454-864X-22-I1-006.

[25] Iacs, *Common Structural Rules for Bulk Carriers and Oil Tankers*, 2024.